Modeling chain collisions in vehicular networks with variable penetration rates

Article (Accepted Version)

Modeling Chain Collisions in Vehicular Networks With Variable Penetration Rates

Daxin Tian[a,d], Jianshan Zhou[a,d], Yunpeng Wang[a,d], Zhengguo Sheng[b], Haiying Xia[c], Zhenguo Yi[c]

[a] *Beijing Key Laboratory for Cooperative Vehicle Infrastructure Systems & Safety Control, School of Transportation Science and Engineering, Beihang University, Beijing 100191, China*
[b] *Department of Engineering and Design, the University of Sussex, Richmond 3A09, UK.*
[c] *Research Institute of Highway Ministry Transport, Beijing 100088, China*
[d] *Jiangsu Province Collaborative Innovation Center of Modern Urban Traffic Technologies, No.2 SiPaiLou, Nanjing 210096, China*

Abstract

The vehicular ad hoc network has great potential in traffic change. One of the most important and interesting issues in the research community is the safety evaluation with limited penetration rates of vehicles equipped with inter-vehicular communications. In this paper, a stochastic model is proposed for analyzing the vehicle chain collisions. It takes into account the influences of different penetration rates and distribution of equipped vehicles, the stochastic nature of inter-vehicular distance distribution, and the different kinematic parameters related to driver and vehicle. The usability and accuracy of this model is tested and proved by comparative experiments with Monte Carlo simulations. The collision possibilities of a platoon in different penetration rates and traffic scenarios are also analyzed based on this model. These results are useful to provide theoretical insights into the safety control of a vehicular platoon.

Keywords: vehicular networks, chain collision, penetration rate, stochastic model

1. Introduction

In recent years, the highly advancement of various wireless communication technologies have accelerated the deployment of the advanced transportation information systems (ATIS). Especially, the ongoing development of dedicated short range communication (DSRC) has made the inter-vehicle communication (IVC) and the road-vehicle communication (RVC) feasible. The vehicular ad-hoc networks (VANETs) can support a variety of onboard active safety applications such as the danger warning systems, the collision avoidance systems, the advanced driver assistance systems

and so on [1]. Many significant research projects relevant to vehicular communication have been subsequently launched over the past dozen years. For examples, the Connected Vehicle project undertaken by the U.S. Department of Transportation and the European projects DRIVE C2X and COMeSafety2 all aim to make the transportation systems benefit from the inter-vehicle communications. One of the main concerns in most of those research projects is improving the performance of disseminating safety messages among neighboring vehicles maintaining low latency and high reliability [2]. Although it has been confirmed that inter-vehicle communication is promising to improve the safety of vehicles on roads, the inter-vehicle communication systems should be evaluated at full length for different driving parameters, vehicle-related properties as well as different traffic conditions before being deployed in real-life vehicular environments.

As a typical safety application of inter-vehicle communications, vehicle chain cooperative collision avoidance (CCA) systems or cooperative adaptive cruise control (CACC) systems have recently received much attention [3–5]. A CCA system allows the DSRC equipped vehicles to promptly react in time to the abrupt deceleration of their front vehicles, even though the emergency is out of their sights. Some successful and well known testing work related to CCA applications can be linked California PATH [6, 7]. Although the U.S. government has announced in February 2014 that new light vehicles should be required to equip V2V (vehicle-to-vehicle) communications [8], the ubiquitous deployment of inter-vehicle communications onboard is not likely to be achieved within the next few years. The actual situation is that those equipped and unequipped vehicles would co-exist in general traffic flows [9]. Therefore, it is meaningful to study the vehicle collisions in platoons where only a fraction of vehicles are equipped with inter-vehicle communications. We will explore the collision in a platoon with different penetration rates of vehicular communication unit.

In this work, we present a stochastic model which removes the assumption that all the vehicles install the wireless vehicular communications units. In the model, the kinematic parameters (e.g., velocity and acceleration) of any vehicle in a platoon are not completely independent but influenced to some extent by the preceding vehicle's kinematics, since the driver would make driving decision partially according to the behavior of its leader, which is called as car-following behavior [10, 11]. The driving operation of one vehicle is a function of the kinematic parameters of its preceding vehicle, which is formulated as a car-following model. The model is defined with a linear ordinary

differential equation which can closely model the response of manually driven vehicles [12, 13]. Furthermore, we investigate the vehicle chain collisions in a given platoon, which considers the influences of different penetration rates of inter-vehicle communication, stochastic nature of inter-vehicle distance distribution, and different kinematic parameters related to driver and vehicle. Similarly to some existing studies [9, 12–15], some basic assumptions are also adopted in this paper to make our work tractable: 1) Each of the vehicles in a given platoon is moving in the same direction and cannot reverse its motion or change its lane even when it will collide with its preceding or rear vehicle; 2) Any potential collisions caused by communication device failures or driver faults are ignored. The model is not limited to the assumption that all the vehicles in a platoon being equipped with vehicular communications. Therefore, our work can be treated as a step toward a deep insight into the safety evaluation of vehicle platoons in general mixed-communication environments, which can help to guide an appropriate implementation of vehicular safety control applications when inter-vehicle communications are not ubiquitously deployed.

The remainder of this paper is organized as follows. A brief review on the related work is presented in Section 2. Section 3 presents the basic computation model for the rear-end collision which takes into account the stochastic nature of inter-vehicular distance distribution and the heterogeneity of vehicle platoon. In Section 4, based on the proposed computation model, we present a Markov chain-based approach for the computation of average collision percentage in a platoon. Section 5 demonstrates the validation and application of our model with different penetration rates, inter-vehicular broadcasting latencies, driver reaction times and kinematic parameters. Finally, concluding remarks are given in Section 6.

2. Related Work

As one of specific and typical issues on traffic safety, vehicle chain collision avoidance has attracted a number of research efforts, and the safety control of automatic vehicle platoons has been modeled as inter-connection systems with wireless vehicular communications. Many researchers have investigated the advanced control policies of vehicle platoons with string stability analysis [12, 13, 16–19]. In their control models, the initial velocity and the inter-vehicle distance are almost assumed to be identical. But, in fact, the inter-vehicle distance between any adjacent vehicles always follows a specific stochastic distribution in most traffic scenarios. Namely, the inter-distance

in a platoon can be reasonably regarded as a random variable when exploring the potential chain collisions. At this point, deterministic formulations in the form of transfer functions used in the aforementioned string ability analysis will be unsuitable to model chain collisions in terms of the stochastic nature of vehicle collisions.

In terms of the stochastic distribution of vehicles in a platoon, a stochastic model is more effective to describe the potential chain collisions. Recently, the evaluation of chain collisions in vehicular communication environments based on stochastic models can be found in [14, 20, 21]. [20, 21] have considered the random braking in their model. Similarly, [14] has proposed a stochastic model for evaluating all the possibilities of chain collisions that may occur in a platoon. The authors focus on the theoretical computation of the collision probability and the expected collision number. In their stochastic model, a more realistic assumption that the inter-distance between vehicles is a random variable is added as well. In addition, in [14], the kinematic parameters of any one vehicle are assumed to be independent from each other's. Compared to most of the aforementioned work, although we also adopt the stochastic model approach, unlike [14, 20, 21], our model removes the assumption that wireless vehicular communications are ubiquitously required for all the vehicles in a platoon. We provide a stochastic model in the context of heterogeneous platoons, in which only partial vehicles are equipped with inter-vehicle communications and they are stochastically distributed. Additionally, one another main difference between this work and the aforementioned lies in the adopted kinematic equation for the description of each vehicle's mobility. In a platoon, the kinematic parameters (e.g., velocity and acceleration) of any one vehicle are not completely independent but influenced to some extent by the preceding vehicle's kinematics, since the driver would make driving decision partially according to the driving operations of its leader in real-life scenarios. This is so-called car-following behavior. Unlike [14] that develops their model on the basis of the simple and independent equation of motion with constant acceleration, we introduce the car-following behavior in the analysis of chain collisions instead. From this view of point, our model offers a more significant insight into the influence of car-following behavior on the heterogeneous platoon safety in a more realistic context. In our model, the driving operation of one vehicle is a function of the kinematic parameters of the preceding vehicle, which is formulated as a typical car-following model [11]. This car-following model is presented as a linear ordinary differential equation, and is validated by [11] through rigorous theoretical analysis and realistic experiments.

But, just for the sake of example, we point out that our stochastic model is independent of the car-following model so that other more complex car-following models can also be substituted into our model.

On the other hand, the authors in [12, 13] focus on the automation of vehicles and have studied the influence of those mixed manual and semi-automated vehicles on the characteristics of general traffic flows. However, as [9] has pointed out, both [12] and [13] do not adopt the assumption of inter-vehicle communications. Namely, their goal does not lay in the context of wireless vehicular communications. The analysis approach adopted in [9] is similar to [12, 13], the more realistic scenarios where a fraction of vehicles in a platoon equips with inter-vehicle communications are investigated, and the Laplace transform is used to formulate the transfer function of the heterogeneous platoon system. However, Chakravarthy et al's model will fail to describe the chain collisions of vehicles whose inter-distance is considered to follow a stochastic distribution. In order to compute their model, the authors require that the inter-vehicle distance between vehicles should be determinedly identical. In fact, this assumption is not realistic in most traffic scenarios as aforementioned. Although our goal of model also focuses on the mixed-communication conditions, unlike [9], our model is stochastic so that it can deal with the stochastic nature of the inter-vehicle distance distribution in heterogeneous platoons and is relatively more appropriate for evaluating the realistic situations.

In this paper, we propose a stochastic model as well as develop a computing paradigm for evaluating the collision probability in a heterogeneous platoon under various impacts. The main novel contributions of our work are threefold: (i) our proposed model deals with the heterogeneity of the vehicle platoon where only partial vehicles are equipped with inter-vehicle communications and stochastically distributed; (ii) this model enables the computation of mixed vehicle chain collisions when taking into account the stochastic nature of the inter-vehicle distance distribution and the effect of car-following behavior; and (iii) as the application of the model, it can provide the quantitative aspects of collision possibility of the overall heterogeneous platoon with respect to different traffic conditions, penetration rates, communication delays and driving parameters. Therefore, the proposed model as well as its computing paradigm can be treated as the supplementary approach to help evaluate vehicle platoon safety and assist the design of safety applications and the traffic management.

3. Basic computation for vehicle collisions

3.1. Description of a vehicle platoon

In this paper, we model a general vehicle platoon moving on a single lane in the same direction as a set $\mathbb{V}$, and $|\mathbb{V}| = N + 1$ $(N > 1)$. A basic assumption adopted here is that any vehicle $V_i \in \mathbb{V}$ $(i = 0, 1, \cdots, N)$ is not allowed to change its direction or its lane even when it will collide with its preceding vehicle or be crashed by its rear one. Thus, the motion trail of each vehicle in this platoon is simplified to be a one-dimensional line. What's more, we consider that there are a certain fraction of vehicles equipped with inter-vehicular communications which are stochastically distributed in this given platoon. For simplicity, we denote those equipped vehicles as a subset $\mathbb{V}_E \subset \mathbb{V}$ and those unequipped vehicles in the same platoon as $\mathbb{V}_U \subset \mathbb{V}$. It can be obviously seen that $\mathbb{V} = \mathbb{V}_E \bigcup \mathbb{V}_U$ and $\mathbb{V}_E \bigcap \mathbb{V}_U = \emptyset$. Some significant timing factors are considered in this paper when a vehicle brakes in response to an emergency. A series of events will successively occur when a vehicle slows down or stop. These successive events are called as the ''timing events'' in [22]. The time to slow down or stop an unequipped vehicle V_i is τ_i. Then, according to [22], this timing parameter τ_i can be dissected as

$$\tau_i = \kappa_i + \epsilon_i + \varepsilon_i \tag{1}$$

where κ_i is the driver perception time, ϵ_i is the driver reaction time, and ε_i is the vehicle deceleration time. Similarly, if one vehicle is equipped with some advanced features such as emergency warning system that is supported by inter-vehicular communication, the driver is able to receive an early emergency warning broadcasted from another preceding equipped vehicle via vehicular wireless communication. In this way, even when the emergency is out of the scope of the driver's sight, this vehicle can react to this collision threat ahead of time when compared to some preceding unequipped vehicles in the same platoon. In this paper, we assume that the warning message is broadcasted via one single hop between any two successive equipped vehicles in the same platoon. The driver of an equipped vehicle can sense the emergency via vehicular communication instead of visual perception. Thus, the time interval an equipped vehicle V_j takes from the moment when the warning message is broadcasted by its previous equipped vehicle to the time when it begins slowing down can be simply dissected as

$$\delta_j = \gamma_j + \epsilon_j + \varepsilon_j \tag{2}$$

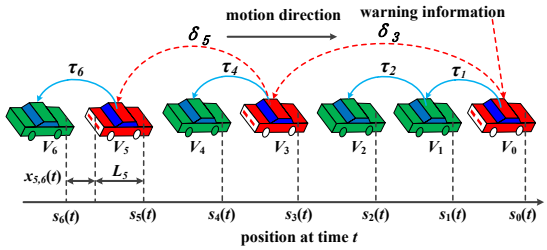

Figure 1 An example for a platoon where those equipped vehicles are marked in red while those unequipped vehicles in green.

where γ_j is the inter-vehicular communication time, ϵ_j is the driver reaction time, and ε_j is the vehicle deceleration time (it is worth pointing out that the vehicle deceleration time ε_j denotes the reaction latency of the vehicular braking system). Actually, the inter-vehicular communication time consists of two main factors that have influence on the timing of emergency perception. As [22] suggested, these factors include the data transmission and broadcasting latencies between vehicular DSRC-based devices. That is, the communication time γ_j can be further expressed as

$$\gamma_j = \gamma_j^{(1)} + \gamma_j^{(2)} \tag{3}$$

where $\gamma_j^{(1)}$ is the transmission latency and $\gamma_j^{(2)}$ is the broadcasting latency. Generally, the time for exchanging a data packet between two equipped vehicles within communication range is in milliseconds, and it would vary from time to time comprehensively depending on the load of wireless communication channels, the density of connected vehicles and the time to digitaly transmit the data packet. More detailed discussion on the timing factors related to vehicular communication as well as the efficiency of DSRC-based communication device can be found in [22, 23].

Consider a vehicle platoon shown in Fig.1 where we assume its leader V_0 is an equipped vehicle that starts braking at the initial time $t_0^b = 0$ due to sensing an emergency in front on the road. Then the emergency warning message is immediately transmitted to the following equipped vehicles via multiple hops. At this point, the time t_j^b for an equipped vehicle $V_j \in \mathbb{V}_E$ to begin deceleration can be accumulatively computed as follows:

$$t_j^b = \sum_{1 \le l \le j-1, V_l \in \mathbb{V}_E} \gamma_l + \delta_j \tag{4}$$

In comparison to those equipped vehicles, those unequipped can only start their deceleration according to the status of the braking light of the preceding vehicles. Thus, the time t_i^b for an

unequipped vehicle $V_i \in \mathbb{V}_U$ to begin braking is

$$t_i^b = t_{j^*}^b + \sum_{j^*+1 \le l \le i, V_l \in \mathbb{V}_U} \tau_l \tag{5}$$

where V_{j^*} is the nearest equipped vehicle in front of the unequipped one V_i. This means that those vehicles located between V_{j^*} and V_i are all unequipped.

From the equations (4) and (5), it can be found that an unequipped vehicle back in the platoon (which means that it is assigned with a larger index) could start braking earlier than a preceding unequipped one. For instance, the vehicle V_4 in Fig.1 will start braking at $t_4^b = t_3^b + \tau_4$ while V_2 at $t_2^b = t_0^b + \tau_1 + \tau_2$, and t_4^b could be smaller than t_2^b when given δ_3 is much smaller than τ_1 and τ_2. At this point, the fact shown in Fig.1 implies that the penetration rate and distribution of those equipped vehicles in a vehicle platoon significantly affects the potential of inter-vehicular collisions.

We define the length of a vehicle $V_i \in \mathbb{V}$ as L_i, and the velocity at time t as $v_i(t)$. Here, we assume that all the vehicles in the given platoon share the same coordinate system. In this coordinate system, the position of a vehicle V_i at time t can be denoted as $s_i(t)$. The space headway between any two adjacent vehicles V_i and V_{i+1} at time t can be calculated as $s_i(t) - s_{i+1}(t)$ (it should be noted that the space headway between vehicles represents the distance from the front bumper of the preceding vehicle to that of the rear one). With these notations, the inter-vehicular distance between V_i and V_{i+1} at time t can be calculated as $x_{i,i+1}(t) = s_i(t) - L_i - s_{i+1}(t)$. Thus, if a rear-end collision occurs between V_i and V_{i+1} at time t, the inter-vehicular distance $x_{i,i+1}(t)$ will satisfy $x_{i,i+1}(t) \le 0$. For simplicity, we assume that the length of every vehicle is equal to L, i.e. $L_i = L$ for $\forall V_i \in \mathbb{V}$. Also, we assume that the overall platoon stays in a stable state at the beginning time $t = 0$. So, every vehicle is assumed to has the same initial velocity v_0, i.e. $v_i(0) = v_0$ for $\forall V_i \in \mathbb{V}$.

3.2. Formulation of vehicle motion

With the help of DSRC system, an equipped vehicle can independently and early start braking after it receives a warning message, while an unequipped one can not sense the existing emergency out of the scope of visual perception, and it can only depend on the velocity of its preceding vehicle or the inter-vehicular distance to slow down once it is aware of the brake light flashing ahead. At this point, we are allowed to assume that the reaction of the driver of an equipped vehicle is independent of the motion state of its preceding vehicle with the assistance of the DSRC,

and this equipped vehicle will start a braking after being informed of an emergency, even when its preceding vehicle has not yet started braking. Additionally, we must point out that in an actual scenario, there exist many factors such as the road surface condition, the road slop, vehicular load, brake lining condition and other complex mechanical factors that should be taken into account to determine the deceleration rate of a vehicle. And the deceleration of the vehicle could be varying during braking. That is, when a driver of a equipped vehicle is informed of the emergency via the inter-vehicular communication system, he/she may operate a moderate brake instead of braking maximally at the beginning, while this driver may increase the deceleration (via increasing the force acting on the brake pedal) after the inter-vehicular distance is obviously shorten and the urgency of the potential rear-end collision is strengthen. In this situation, the deceleration of this vehicle is changing along with the variation of the force acting on the brake pedal. Consequently, the potential manual factor increases the complexity of modeling the vehicle motion. To make our work tractable but without loss of practical meaning, we present the deceleration of those equipped vehicles $V_j \in \mathbb{V}_E$ as a constant a_j. The similar model for describing the movement of an equipped vehicle and the assumption of operating a constant deceleration are also used in other research works such as [14, 24–26]. The braking process of those equipped vehicles is approximated by the uniformly retarded motion, which can be defined as:

$$v_j(t) = \begin{cases} v_0, & 0 \leq t < t_j^b \\ v_0 + a_j(t - t_j^b), & t_j^b \leq t < (t_j^b + \dfrac{-v_0}{a_j}) \\ 0, & t \geq (t_j^b + \dfrac{-v_0}{a_j}) \end{cases} \tag{6}$$

where a_j is the deceleration of the equipped vehicle V_j and its algebra value is negative, i.e. $a_j < 0$. If it does not collide, the maximum distance traveled by V_j can be calculated as

$$d_j^{max} = t_j^b v_0 - \frac{{v_0}^2}{2a_j} \tag{7}$$

In order to demonstrate the validity of the aforementioned model, we compare the stopping distance calculated by equation (7) with the actual testing results obtained in the work of [22]. They adopted the car model manufactured by GM to explore the rear-end collision and intersection collision with DSRC-based inter-vehicular communication systems. We adopt the poorer manufacturer-tested braking conditions which has more practical significance to the design of some vehicular safety applications, the relevant data can be found in Table 2 in Appendix A of [22]. In

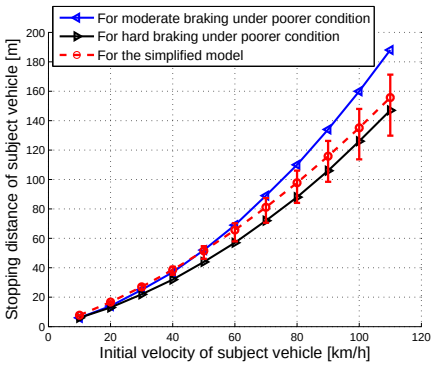

Figure 2 Comparing the equipped vehicle stopping distance under the manufacture-tested conditions with that obtained by (7).

the experiment, the vehicle response time is set at 50ms and the driver perception and reaction time at 2.5s, the average deceleration of the hard braking is -6m/s^2, the initial velocity varies from 10km/h to 110km/h. In addition, to provide the upper and lower bounds of the stopping distance obtained by the proposed motion model at each velocity point, we also assume that the deceleration adopted is always bounded within $[-7.5, -4.5]\text{m/s}^2$. Then, we use the equation (7) to calculate the average stopping distance and its upper and lower bounds corresponding to each initial velocity. The comparative results are shown in Fig.2. It should be noted that the upper and lower bounds of the result at each velocity point are obtained by (7) with two settings $a_j = -4.5\text{m/s}^2$ and $a_j = -7.5\text{m/s}^2$, respectively. And they are presented by the upper and lower ends of the corresponding error bar in Fig.2.

From Fig.2, it can be found that the result obtained by equation (7) is almost between those obtained in moderate braking and hard braking, and closer to the actual testing result of hard braking under poorer condition. And more importantly, the upper bound of the defined model is also near the testing result in moderate braking, and the lower bound contains the testing result obtained in the hard braking situation. This means that the model can approximate the actual result of braking with varying deceleration (as concerned in real-world situations). Therefore, the adopted model with the setting $a_j \in [-7.5, -4.5]\text{m/s}^2$ is reasonable enough to approximate the actual braking situation in real world. In the following experiments, the independent deceleration of every equipped vehicle is bounded within $[-7.5, -4.5]\text{m/s}^2$.

Next, we come to model the motion of those unequipped vehicles. Since an unequipped vehicle's motion depending on the behavior of the nearest preceding vehicle, its movement is modeled by

the car-following approach proposed in [10, 11]. This car-following model can give a smooth approximation of the manual driving response and has been used for the mixed manual and semi-automated vehicle simulations in [12, 13]. Consider that an unequipped vehicle $V_i \in \mathbb{V}_U$ follows its nearest preceding vehicle V_{i-1}. Then, according to the car-following model, the response of V_i can be defined as

$$\frac{\mathrm{d}v_i(t)}{\mathrm{d}t} = \mu_i \times (v_{i-1}(t-\tau_i) - v_i(t-\tau_i)) \times u\,(t-\tau_i) \tag{8}$$

where μ_i is a sensitivity factor, and $u(t-\tau_i)$ is an indicator function that is given by

$$u(t-\tau_i) = \begin{cases} 1, & t > \tau_i \\ 0, & t \leq \tau_i \end{cases} \tag{9}$$

In equation (8), the reaction of the unequipped vehicle V_i is a function of its own parameters and those of the preceding vehicle V_{i-1}. That is, its velocity in a given vehicle platoon at time t should be computed recursively by taking the integral

$$v_i(t) = v_0 + \int_0^t \frac{\mathrm{d}v_i(l)}{\mathrm{d}l}\mathrm{d}l = v_0 + \int_{\tau_i}^t \mu_i \times (v_{i-1}(l-\tau_i) - v_i(l-\tau_i))\,\mathrm{d}l \tag{10}$$

3.3. Collision computation model

Consider that those equipped and unequipped vehicles are stochastically mixed in the same platoon as shown in Fig.1. All the possible car-following situations can be summed up as four cases (see Fig.3). In the first case, the preceding vehicle is considered to be an equipped while the rear one is unequipped. The second case is contrary to this case, in which the forward is an unequipped vehicle but the follower is an equipped one. In the third case, both vehicles are equipped. And both vehicles are unequipped in the fourth case. Based on this, we are allowed to investigate the possibility of a collision occurring between any two adjacent vehicles. When a rear vehicle is unequipped as the first and the fourth cases illustrate, it can only follow its preceding vehicle to brake after being aware of the flashing brake light of the preceding vehicle. If there is not enough time for slowing the rear vehicle safely, a collision may occur in this situation. In the third case, although both the equipped vehicles are assumed to independently decelerate with the assistance of the inter-vehicular communication system, a potential collision also exists. This is because the magnitude of the deceleration of the rear vehicle may be smaller than the forward's. In the second case where an equipped vehicle follows an unequipped, the rear equipped vehicle

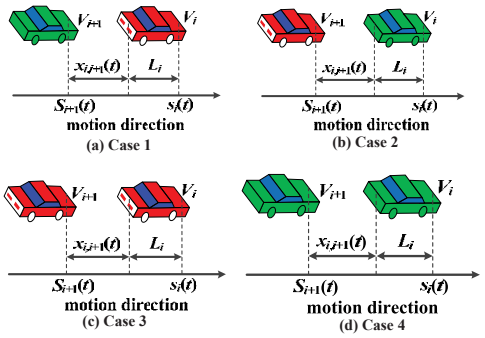

Figure 3 All the possible car-following cases between adjacent vehicles, the equipped vehicle is red and the unequipped one is green.

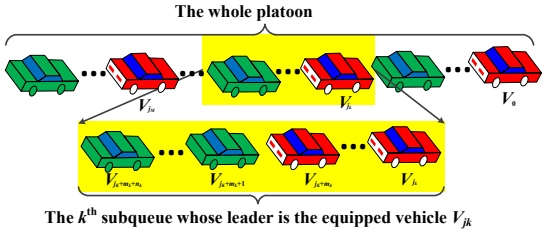

Figure 4 An example of a subqueue.

usually responds to the emergency much earlier than the preceding vehicle. Recalling that we have assumed the equipped vehicle independently decelerates in a hard braking manner, we further assume this equipped vehicle does not crash into the preceding unequipped one.

Based on the above discussion, we are allowed to simplify the overall platoon by dividing the overall platoon into a series of subqueues. The leader of each subqueue is an equipped vehicle while its successive followers could be equipped ones or unequipped. And the vehicle in front of each subqueue leader is unequipped. Let $M+1$ be the total number of the subqueues. The equipped leader of the k-th subqueue is denoted as $V_{j_k} \in \mathbb{V}_E (k = 0, 1, \ldots, M)$. Furthermore, we assume that there are m_k successive equipped vehicles and n_k unequipped vehicles following V_{j_k} in the k-th subqueue. That is, we have $V_{j_k}, V_{j_k+1}, \ldots, V_{j_k+m_k} \in \mathbb{V}_E$ and $V_{j_k+m_k+1}, V_{j_k+m_k+2}, \ldots, V_{j_k+m_k+n_k} \in \mathbb{V}_U$, see Fig. 4.

To derive our basic collision computation model, we first introduce the assumption that if any two adjacent vehicles are collided with each other, they will stop immediately at the position where the collision occurs. This assumption neglects the effect of the momentum conservation law on the

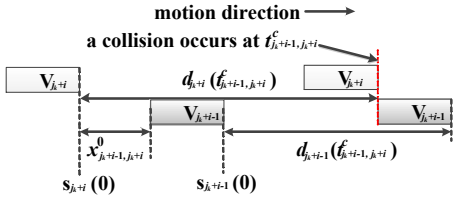

Figure 5 The positional relationship between V_{j_k+i-1} and V_{j_k+i} when a rear-end collision occurs.

motion of two crashed vehicles for the sake of simplicity. It is worth pointing out that this assumption has also been adopted in other existing works such as [14, 20], which allows one to evaluate the worst collision situation. Since the overall platoon is divided into a series of subqueues, we turn to focus on a subqueue denoted as the set $\{V_{j_k}, V_{j_k+1}, \ldots, V_{j_k+m_k}, V_{j_k+m_k+1}, \ldots, V_{j_k+m_k+n_k}\}$ where $V_{j_k}, V_{j_k+1}, \ldots, V_{j_k+m_k} \in \mathbb{V}_E$ and

$V_{j_k+m_k+1}, \ldots, V_{j_k+m_k+n_k} \in \mathbb{V}_U$. Let the initial inter-vehicular distance between any adjacent vehicles V_{j_k+i-1} and V_{j_k+i} be $x^0_{j_k+i-1,j_k+i} = x_{j_k+i-1,j_k+i}(0)(i = 1, 2, \ldots, m_k + n_k)$ and the distance traveled by V_{j_k+i} by the time t be $d_{j_k+i}(t)(i = 0, 1, \ldots, m_k + n_k)$. Thus, a sufficient and necessary condition for determining a rear-end collision between two adjacent vehicles V_{j_k+i-1} and V_{j_k+i} can be mathematically defined as

$$\max_{t\in[0,+\infty)} \{d_{j_k+i}(t) - d_{j_k+i-1}(t)\} \geq x^0_{j_k+i-1,j_k+i} \tag{11}$$

If a rear-end collision is considered to occur between V_{j_k+i-1} and V_{j_k+i} (see Fig.5), the time instant of the collision occuring is defined as $t^c_{j_k+i-1,j_k+i}$, which is a finite positive real number, i.e. $t^c_{j_k+i-1,j_k+i} \in (0, +\infty)$.

In the equation (11), it can be found that the initial inter-vehicular distance is one of the most significant parameters to determine the vehicle collision. Generally, those equipped and unequipped vehicles are considered to stochastically distribute in one platoon, and the space headway between vehicles always follows a certain stochastic distribution. Therefore, the inter-vehicular distance should also be a random variable following the same stochastic distribution when every vehicle has a constant length. The exponential distribution assumption has been widely used in many recent works such as [27–30]. In this paper, we also assume that the space headways in the given platoon follow an exponential distribution so that the initial inter-vehicular distance $x^0_{j_k+i-1,j_k+i}$ is an exponentially distributed random variable. Let this exponential distribution be characterized with the parameter ρ. Then, we have $x^0_{j_k+i-1,j_k+i} \sim \exp(\rho)$ for $i = 1, 2, \ldots, m_k + n_k$ and $k = 0, 1, \ldots, M$.

ρ represents the density of the traffic flow on the road whose unit is veh/m. The corresponding probability density function (pdf) is

$$f(x;\rho)=\begin{cases}\rho e^{-\rho x}, & x>0\\ 0, & x\leq 0\end{cases} \tag{12}$$

It is worth pointing out that the inter-vehicular distance in different traffic flows will follow different stochastic distributions. The exponential distribution adopted in this paper is not unique. Once other specific formulation of the pdf of the inter-vehicular distance distribution is derived, it can be used to substitute the exponential pdf. That is, our model is independent of the specific inter-vehicular distance distribution.

In a given subqueue, the probability $p^{(1)}_{j_k+i-1,j_k+i}$ that the rear vehicle V_{j_k+i} does not crash into its preceding vehicle V_{j_k+i-1} $(i=1,2,\ldots,m_k+n_k)$ can be calculated as follows:

$$\begin{aligned}p^{(1)}_{j_k+i-1,j_k+i}&=1-Pro\left\{\Delta d^{*}_{j_k+i-1,j_k+i}\geq x^{0}_{j_k+i-1,j_k+i}\right\}\\&=1-\int_{-\infty}^{\Delta d^{*}_{j_k+i-1,j_k+i}} f(x;\rho)\mathrm{d}x=1-\int_{0}^{\Delta d^{*}_{j_k+i-1,j_k+i}} \rho e^{-\rho x}\mathrm{d}x=e^{-\rho\Delta d^{*}_{j_k+i-1,j_k+i}}\end{aligned} \tag{13}$$

And the corresponding inter-vehicular collision probability $p^{(2)}_{j_k+i-1,j_k+i}$ is derived as

$$p^{(2)}_{j_k+i-1,j_k+i}=1-p^{(1)}_{j_k+i-1,j_k+i} \tag{14}$$

In the equation (13), the parameter $\Delta d^{*}_{j_k+i-1,j_k+i}$ is set to the maximum relative inter-vehicular distance, i.e. $\Delta d^{*}_{j_k+i-1,j_k+i}=\max_{t\in[0,+\infty)}\left\{d_{j_k+i}(t)-d_{j_k+i-1}(t)\right\}$.

From the equations (11) and (13), it can be found that the maximum relative inter-vehicular distance $\Delta d^{*}_{j_k+i-1,j_k+i}$ should be determined before deriving $p^{(1)}_{j_k+i-1,j_k+i}$ and $p^{(2)}_{j_k+i-1,j_k+i}$. However, when considering the initial inter-vehicular distance follows the stochastic distribution, it is not tractable to deterministically calculate $\Delta d^{*}_{j_k+i-1,j_k+i}$. Even it is difficult to directly derive $d_{j_k+i-1}(t)$ and $d_{j_k+i}(t)$. Therefore, to make the computation tractable, we resort to the concept of the mathematical expectation in probability theory so as to define our stochastic model. We calculate the expected value $E[d_{j_k+i}(t^{s}_{j_k+i})]$ of the total distance $d_{j_k+i}(t^{s}_{j_k+i})$ traveled by any vehicle $V_{j_k+i}(i=0,1,\ldots,m_k+n_k)$ when it stops at time $t^{s}_{j_k+i}$ as well as the expected relative distance $E(\Delta d_{j_k+i_k-1,j_k+i_k})$ between any two adjacent vehicles V_{j_k+i-1} and V_{j_k+i}. For simplicity, let $\overline{d}_{j_k+i}=E[d_{j_k+i}(t^{s}_{j_k+i})]$ and $\Delta\overline{d}_{j_k+i-1,j_k+i}=E(\Delta d_{j_k+i_k-1,j_k+i_k})$. As the subqueue example shown in Fig.4, there are only three car-following situations (shown by Case 1,

Case 3 and Case 4 in Fig.3) possibly involved in a subqueue. Accordingly, the subqueue can further be divided into two parts, one of which comprises those successive equipped vehicles $\{V_{j_k}, V_{j_k+1}, \ldots, V_{j_k+m_k}\} \subset \mathbb{V}_E$ in the front of this subqueue, the other comprises those rear unequipped vehicles $\{V_{j_k+m_k+1}, V_{j_k+m_k+2}, \ldots, V_{j_k+m_k+n_k}\}$. Therefore, we can consider two situations in detail, respectively.

3.3.1. Collision computation model if the rear vehicle is equipped

In the first situation, consider an equipped vehicle V_{j_k+j} that follows another equipped vehicle $V_{j_k+j-1}(1 \leq j \leq m_k)$. Through equation (7), it can be known that the distance $d_{j_k+j}(t^s_{j_k+j})$ traveled by V_{j_k+j} attains the maximum value $d^{max}_{j_k+j}$ when giving V_{j_k+j} does not collide with V_{j_k+j-1} and normally stops at time $t^s_{j_k+j}$. If given the expected distance $\overline{d}_{j_k+j-1}$ traveled by V_{j_k+j-1}, we can approximate the maximum relative distance between V_{j_k+j-1} and V_{j_k+j} as:

$$\Delta d^*_{j_k+j-1,j_k+j} = d^{max}_{j_k+j} - \overline{d}_{j_k+j-1} \tag{15}$$

By substituting the result of the equation (15) into the equation (13), the probabilities $p^{(1)}_{j_k+j-1,j_k+j}$ and $p^{(2)}_{j_k+j-1,j_k+j}$ can be derived.

On the other hand, according to the definition of the expected value, the expected distance $\overline{d}_{j_k+j}$ traveled by the rear vehicle V_{j_k+j} can be calculated by the probability-weighted average of all possible values of $d_{j_k+j}(t^s_{j_k+j})$. Thus, we get

$$\overline{d}_{j_k+j} = p^{(1)}_{j_k+j-1,j_k+j} \times d^{max}_{j_k+j} + p^{(2)}_{j_k+j-1,j_k+j} \times \overline{d}^{c}_{j_k+j} \tag{16}$$

where $\overline{d}^{c}_{j_k+j}$ is the expected distance traveled by V_{j_k+j} by the time when it is considered to collide with V_{j_k+j-1}.

More specifically, recalling that these two adjacent equipped vehicles have the same initial velocity and independently decelerate, these two vehicles may collide in three ways: i) *the preceding vehicle is braking while the rear keeps traveling*; ii) *both vehicles are braking*; and iii) *the preceding vehicle has stopped*. Each of those rear-end collision ways could lead to a different expected distance $\overline{d}^{c}_{j_k+j}$ traveled by V_{j_k+j}. For convenience of discussion, we first denote $\overline{d}^{c1}_{j_k+j}$ that is the expected distance traveled by V_{j_k+j} to stop when considering the rear-end collision occurs in the way i), $\overline{d}^{c2}_{j_k+j}$ corresponding to ii) and $\overline{d}^{c3}_{j_k+j}$ to iii). Furthermore, the probability of the rear-end collision occurring in those three ways are denoted as $p^{c1}_{j_k+j-1,j_k+j}$, $p^{c2}_{j_k+j-1,j_k+j}$ and $p^{c3}_{j_k+j-1,j_k+j}$,

respectively. Subsequently, we can replace the term $p^{(2)}_{j_k+j-1,j_k+j} \times d^c_{j_k+j}$ in the equation (16) by using those different expected distances to stop as follows

$$\overline{d}_{j_k+j} = p^{(1)}_{j_k+j-1,j_k+j} \times d^{max}_{j_k+j} + p^{c1}_{j_k+j-1,j_k+j} \times \overline{d}^{c1}_{j_k+j} + p^{c2}_{j_k+j-1,j_k+j} \times \overline{d}^{c2}_{j_k+j} + p^{c3}_{j_k+j-1,j_k+j} \times \overline{d}^{c3}_{j_k+j} \quad (17)$$

Through equation (17), we can approximate the distance traveled by an equipped vehicle by the time when it stops in the sense of the mathematical expectation. This approximation is reasonable since it takes into account the stochastic nature of the inter-vehicular distance distribution and the similar computation technique has also been adopted in the work of [14, 26].

By referring to the computation formula of the mathematical expectation in the probability theory, we can present the general formula for computing the expected distance as follows:

$$\overline{dist}_{j_k+j} = \frac{1}{\int_{\Omega_L} f(l;\rho)\mathrm{d}l} \int_{\Omega_L} dist_{j_k+j}(l) \times f(l;\rho)\mathrm{d}l \quad (18)$$

where $dist_{j_k+j}(l)$ is the distance to stop traveled by the vehicle V_{j_k+j} when given the initial inter-vehicular distance between V_{j_k+j-1} and V_{j_k+j} is the random variable l, $\overline{dist}_{j_k+j}$ is the corresponding expected distance and $f(l;\rho)$ is the probability density function of l. Ω_L denotes the value space of l. By following (18), we can derive the computation models of $\overline{d}^{c1}_{j_k+j}$, $\overline{d}^{c2}_{j_k+j}$ and $\overline{d}^{c3}_{j_k+j}$ respectively as follows:

For proceeding the derivation, we firstly introduce some time notations including $t^s_{j_k+j-1}$ and $t_{j_k+j}(l)$. $t^s_{j_k+j-1}$ is defined as the time spent by the vehicle V_{j_k+j-1} to travel the expected distance $\overline{d}_{j_k+j-1}$ to stop. $t_{j_k+j}(l)$ represents the time instant at which the rear-end collision occurs in the ii) way mentioned before, where the initial inter-vehicular distance between V_{j_k+j-1} and V_{j_k+j} is l. Let $tim^s_{j_k+j}(l)$ represent the time spent by the vehicle V_{j_k+j} to travel the distance l. Then, $tim^s_{j_k+j}(l)(\text{for} j = 0, 1, \ldots, m_k)$ can be calculated as

$$tim^s_{j_k+j}(l) = \begin{cases} \dfrac{l}{v_0}, & 0 \le l \le v_0 t^b_{j_k+j} \\ t^b_{j_k+j} - \dfrac{v_0}{a_{j_k+j}} - \sqrt{\dfrac{2}{a_{j_k+j}}(l - d^{max}_{j_k+j})}, & v_0 t^b_{j_k+j} < l \le d^{max}_{j_k+j} \end{cases} \quad (19)$$

Hence, we can derive $t^s_{j_k+j-1} = tim^s_{j_k+j-1}(\overline{d}_{j_k+j-1})$.

A. When considering V_{j_k+j-1} is braking while V_{j_k+j} keeps traveling with the constant velocity

In this situation, it implies that the time instant when the preceding vehicle V_{j_k+j-1} stops should not be less than the time instant at which this vehicle starts braking, i.e., $t^s_{j_k+j-1} \le t^b_{j_k+j-1}$. Thus,

when $t^s_{j_k+j-1} > t^b_{j_k+j-1}$, we can simply set $\overline{d}^{c1}_{j_k+j} = 0$. Otherwise, a time instant must exist when V_{j_k+j} crashes into V_{j_k+j-1}. Given an initial inter-vehicular distance $x^0_{j_k+j-1,j_k+j}$ (for simplicity, we use l to substitute the notation $x^0_{j_k+j-1,j_k+j}$ in the following discussion), we denote this time instant as $t_{j_k+j}(l)$, and it should satisfy

$$t^b_{j_k+j-1} \leq t_{j_k+j}(l) \leq \min\left\{t^s_{j_k+j-1}, t^b_{j_k+j}\right\} \tag{20}$$

and

$$v_0 t_{j_k+j}(l) = l + v_0 t_{j_k+j}(l) + \frac{1}{2} a_{j_k+j-1}(t_{j_k+j}(l) - t^b_{j_k+j-1})^2 \tag{21}$$

Thus, from the equation (21), we can further get

$$l = -\frac{1}{2} a_{j_k+j-1}(t_{j_k+j}(l) - t^b_{j_k+j-1})^2 \tag{22}$$

Accordingly, we can get the upper and lower bounds $L_1^{\min}$, $L_1^{\max}$ for l by substituting the bounds of $t_{j_k+j}(l)$ into the equation (22) so as to get

$$L_1^{\min} = -\frac{1}{2} a_{j_k+j-1}(t^b_{j_k+j-1} - t^b_{j_k+j-1})^2 = 0 \tag{23}$$

$$\begin{aligned} L_1^{\max} &= -\frac{1}{2} a_{j_k+j-1} \min\left\{(t^s_{j_k+j-1} - t^b_{j_k+j-1})^2, (t^b_{j_k+j} - t^b_{j_k+j-1})^2\right\} \\ &= -\frac{1}{2} a_{j_k+j-1} \min\left\{(t^s_{j_k+j-1} - t^b_{j_k+j-1})^2, \delta^2_{j_k+j}\right\} \end{aligned} \tag{24}$$

By solving (22), we get

$$t_{j_k+j}(l) = \sqrt{\frac{-2l}{a_{j_k+j-1}}} + t^b_{j_k+j-1} \tag{25}$$

Then, substituting the result of (25) into the term $v_0 t_{j_k+j}(l)$, we can obtain the distance traveled by V_{j_k+j} when given an initial inter-vehicular distance l:

$$dist_{j_k+j}(l) = v_0 \left(\sqrt{\frac{-2l}{a_{j_k+j-1}}} + t^b_{j_k+j-1}\right) \tag{26}$$

Hence, we set the value space as $\Omega_L = \left\{l | \forall l \in [L_1^{\min}, L_1^{\max}]\right\}$ and substitute (26) into the integral (18) to get

$$\overline{d}^{c1}_{j_k+j} = \frac{1}{p^{c1}_{j_k+j-1,j_k+j}} \int_{L_1^{\min}}^{L_1^{\max}} v_0 \left(\sqrt{\frac{-2l}{a_{j_k+j-1}}} + t^b_{j_k+j-1}\right) \rho e^{-\rho l} \mathrm{d}l \tag{27}$$

where $p^{c1}_{j_k+j-1,j_k+j} = \int_{L_1^{\min}}^{L_1^{\max}} \rho e^{-\rho l} \mathrm{d}l$.

B. When considering both vehicles V_{j_k+j-1} and V_{j_k+j} are braking

When a rear-end collision would not occur during both vehicles braking, i.e., $t^s_{j_k+j-1} \leq t^b_{j_k+j-1}$, we can simply set $\overline{d}^{c2}_{j_k+j} = 0$. Otherwise, when a rear-end collision occurs during both vehicles braking, a time instant $t_{j_k+j}(l)$ should exist and satisfy:

$$t^b_{j_k+j-1} \leq t_{j_k+j}(l) \leq t^s_{j_k+j-1} \tag{28}$$

and

$$t^b_{j_k+j} \leq t_{j_k+j}(l) \leq t^b_{j_k+j} - \frac{v_0}{a_{j_k+j}} \tag{29}$$

Based on the definition of $t_{j_k+j}(l)$, the distance traveled by V_{j_k+j} by the time it stops can be yielded as

$$dist_{j_k+j}(l) = v_0 t_{j_k+j}(l) + \frac{1}{2} a_{j_k+j} (t_{j_k+j}(l) - t^b_{j_k+j})^2 \tag{30}$$

By substituting (30) into (18), we can have

$$\overline{d}^{c2}_{j_k+j} = \frac{1}{p^{c2}_{j_k+j-1,j_k+j}} \int_{L_2^{\min}}^{L_2^{\max}} [v_0 t_{j_k+j}(l) + \frac{1}{2} a_{j_k+j} (t_{j_k+j}(l) - t^b_{j_k+j})^2] \rho e^{-\rho l} \mathrm{d}l \tag{31}$$

where the parameters $L_2^{\min}$ and $L_2^{\max}$ are defined as the lower and upper bounds of l in this integral.

Accordingly, we can further represent $\overline{d}^{c2}_{j_k+j}$ as

$$\overline{d}^{c2}_{j_k+j} = \frac{1}{p^{c2}_{j_k+j-1,j_k+j}} \times \begin{cases} 0, & t^s_{j_k+j-1} \leq t^b_{j_k+j-1} \\ \int_{L_2^{\min}}^{L_2^{\max}} [v_0 t_{j_k+j}(l) + \frac{1}{2} a_{j_k+j} (t_{j_k+j}(l) - t^b_{j_k+j})^2] \rho e^{-\rho l} \mathrm{d}l, & t^s_{j_k+j-1} > t^b_{j_k+j-1} \end{cases} \tag{32}$$

Additionally, we discuss the calculations of those parameters $L_2^{\min}$, $L_2^{\max}$ and $t_{j_k+j}(l)$ in three situations where the decelerations a_{j_k+j} and a_{j_k+j-1} may have different relationships: (i) $(a_{j_k+j} - a_{j_k+j-1}) > 0$, (ii) $a_{j_k+j} = a_{j_k+j-1}$ and (iii) $(a_{j_k+j} - a_{j_k+j-1}) < 0$. Recalling $t^b_{j_k+j} = t^b_{j_k+j-1} + \delta_{j_k+j} > t^b_{j_k+j-1}$, we can lump (28) and (29) as

$$t^b_{j_k+j} \leq t_{j_k+j}(l) \leq \min \left\{ t^s_{j_k+j-1}, t^b_{j_k+j} - \frac{v_0}{a_{j_k+j}} \right\} \tag{33}$$

On the other side, this time instant $t_{j_k+j}(l)$ should also satisfy the kinematic relation

$$v_0 t_{j_k+j}(l) + \frac{1}{2} a_{j_k+j} (t_{j_k+j}(l) - t^b_{j_k+j})^2 = l + v_0 t_{j_k+j}(l) + \frac{1}{2} a_{j_k+j-1} (t_{j_k+j}(l) - t^b_{j_k+j-1})^2 \tag{34}$$

By substituting $t^b_{j_k+j} = t^b_{j_k+j-1} + \delta_{j_k+j}$ into (34), we get

$$l = \frac{1}{2} (a_{j_k+j} - a_{j_k+j-1}) (t_{j_k+j}(l) - t^b_{j_k+j-1})^2 - a_{j_k+j} \delta_{j_k+j} (t_{j_k+j}(l) - t^b_{j_k+j-1}) + \frac{1}{2} a_{j_k+j} \delta^2_{j_k+j} \tag{35}$$

The equation (35) above can be treated as a quadratic function of l with respect to $(t_{j_k+j}(l) - t^b_{j_k+j-1})$. For simplifying the mathematical expressions, we denote $x = t_{j_k+j}(l) - t^b_{j_k+j-1}$ and $l = g(x) = \frac{1}{2}(a_{j_k+j} - a_{j_k+j-1})x^2 - a_{j_k+j}\delta_{j_k+j}x + \frac{1}{2}a_{j_k+j}\delta^2_{j_k+j}$. Recalling (33), we can have $t^b_{j_k+j} - t^b_{j_k+j-1} = \delta_{j_k+j} \leq x \leq t^{sup}_{j_k+j}$ where $t^{sup}_{j_k+j} = \min\left\{t^s_{j_k+j-1}, t^b_{j_k+j} - \frac{v_0}{a_{j_k+j}}\right\} - t^b_{j_k+j-1}$.

(i) *When* $(a_{j_k+j} - a_{j_k+j-1}) > 0$, the quadratic function $g(x)$ is the parabola that opens upward and the axis of symmetry (i.e., the x-coordinate of the vertex) of which is $x^* = \frac{a_{j_k+j}\delta_{j_k+j}}{(a_{j_k+j} - a_{j_k+j-1})} < 0$ (noting that $a_{j_k+j} < 0$). Since this quadratic function $g(x)$ will increase with increasing x in the range $[x^*, +\infty)$, we can obtain the minimum and maximum values $L_2^{\min}$, $L_2^{\max}$ of $g(x)$ in the closed interval $[\delta_{j_k+j}, t^{sup}_{j_k+j}] \subset [x^*, +\infty)$ as

$$L_2^{\min} = \frac{1}{2}(a_{j_k+j} - a_{j_k+j-1})\delta^2_{j_k+j} - a_{j_k+j}\delta^2_{j_k+j} + \frac{1}{2}a_{j_k+j}\delta^2_{j_k+j} = -\frac{1}{2}a_{j_k+j-1}\delta^2_{j_k+j} \tag{36}$$

$$L_2^{\max} = g(t^{sup}_{j_k+j}) = \frac{1}{2}(a_{j_k+j} - a_{j_k+j-1})(t^{sup}_{j_k+j})^2 - a_{j_k+j}\delta_{j_k+j}(t^{sup}_{j_k+j}) + \frac{1}{2}a_{j_k+j}\delta^2_{j_k+j} \tag{37}$$

In addition, by solving $l = g(x)$, we can get two real roots:

$$\begin{cases} x_1 = \dfrac{a_{j_k+j}\delta_{j_k+j} + \sqrt{(a_{j_k+j}\delta_{j_k+j})^2 - 2(a_{j_k+j} - a_{j_k+j-1})(\frac{1}{2}a_{j_k+j}\delta^2_{j_k+j} - l)}}{(a_{j_k+j} - a_{j_k+j-1})} \\ x_2 = \dfrac{a_{j_k+j}\delta_{j_k+j} - \sqrt{(a_{j_k+j}\delta_{j_k+j})^2 - 2(a_{j_k+j} - a_{j_k+j-1})(\frac{1}{2}a_{j_k+j}\delta^2_{j_k+j} - l)}}{(a_{j_k+j} - a_{j_k+j-1})} \end{cases} \tag{38}$$

From (38), we can see that $x_2 < 0$ while $x_1 > 0$. At this point, recalling $x = t_{j_k+j}(l) - t^b_{j_k+j-1} \geq \delta_{j_k+j} > 0$, we can get

$$t_{j_k+j}(l) = x_1 + t^b_{j_k+j-1} = \frac{a_{j_k+j}\delta_{j_k+j} + \sqrt{(a_{j_k+j}\delta_{j_k+j})^2 - 2(a_{j_k+j} - a_{j_k+j-1})(\frac{1}{2}a_{j_k+j}\delta^2_{j_k+j} - l)}}{(a_{j_k+j} - a_{j_k+j-1})} + t^b_{j_k+j-1} \tag{39}$$

(ii) *When* $(a_{j_k+j} - a_{j_k+j-1}) = 0$, we are allowed to simplify $l = g(x)$ as a linear function $l = g(x) = -a_{j_k+j}\delta_{j_k+j}x + \frac{1}{2}a_{j_k+j}\delta^2_{j_k+j}$. Since the coefficient $-a_{j_k+j}\delta_{j_k+j} > 0$, $l = g(x)$ is a monotonously increasing function of x. Therefore, it can be obviously obtained that

$$L_2^{\min} = g(\delta_{j_k+j}) = -\frac{1}{2}a_{j_k+j}\delta^2_{j_k+j} \tag{40}$$

and

$$L_2^{\max} = g(t^{sup}_{j_k+j}) = -a_{j_k+j}\delta_{j_k+j}t^{sup}_{j_k+j} + \frac{1}{2}a_{j_k+j}\delta^2_{j_k+j} \tag{41}$$

At the meanwhile, the time instant $t_{j_k+j}(l)$ can be calculated by solving $l = g(x)$:

$$t_{j_k+j}(l) = \frac{\frac{1}{2}a_{j_k+j}\delta_{j_k+j}^2 - l}{a_{j_k+j}\delta_{j_k+j}} + t_{j_k+j-1}^b \tag{42}$$

(iii) *When* $(a_{j_k+j} - a_{j_k+j-1}) < 0$, the quadratic function $l = g(x)$ becomes the parabola that opens downward and the axis of symmetry $x^* = \frac{a_{j_k+j}\delta_{j_k+j}}{(a_{j_k+j}-a_{j_k+j-1})} > \delta_{j_k+j}$. By solving $g(x) = 0$, we can get two square real roots as

$$\begin{cases} r_1 = \dfrac{\sqrt{|a_{j_k+j}|}}{\sqrt{|a_{j_k+j}|} + \sqrt{|a_{j_k+j-1}|}}\delta_{j_k+j} \\ r_2 = \dfrac{-\sqrt{|a_{j_k+j}|}}{\sqrt{|a_{j_k+j-1}|} - \sqrt{|a_{j_k+j}|}}\delta_{j_k+j} \end{cases} \tag{43}$$

From (43), it can be found that $r_1 < \delta_{j_k+j} < r_2$. Thus, in order to guarantee $l = g(x) \geq 0$, the variable x should be limited within $[r_1, r_2]$. In $[r_1, r_2]$, the maximum value of $l = g(x)$ is $\frac{(a_{j_k+j}-a_{j_k+j-1})a_{j_k+j}\delta_{j_k+j}^2 - a_{j_k+j}^2\delta_{j_k+j}^2}{2(a_{j_k+j}-a_{j_k+j-1})}$. Furthermore, since $\delta_{j_k+j} \leq x \leq t_{j_k+j}^{sup}$, $l \geq 0$ holds with the condition $\delta_{j_k+j} \leq x \leq \min\left\{t_{j_k+j}^{sup}, r_2\right\}$. More specifically, if $t_{j_k+j}^{sup} \geq r_2$, we can set

$$\begin{cases} L_2^{\min} = g(r_2) = 0 \\ L_2^{\max} = \dfrac{(a_{j_k+j} - a_{j_k+j-1})a_{j_k+j}\delta_{j_k+j}^2 - a_{j_k+j}^2\delta_{j_k+j}^2}{2(a_{j_k+j} - a_{j_k+j-1})} \end{cases} \tag{44}$$

Otherwise, if $t_{j_k+j}^{sup} < r_2$, we can get

$$L_2^{\min} = \min\left\{g(\delta_{j_k+j}), g(t_{j_k+j}^{sup})\right\} = \min\left\{-\frac{1}{2}a_{j_k+j-1}\delta_{j_k+j}^2, g(t_{j_k+j}^{sup})\right\} \tag{45}$$

$$L_2^{\max} = \begin{cases} g(t_{j_k+j}^{sup}), & t_{j_k+j}^{sup} \leq x^* \\ \dfrac{(a_{j_k+j} - a_{j_k+j-1})a_{j_k+j}\delta_{j_k+j}^2 - a_{j_k+j}^2\delta_{j_k+j}^2}{2(a_{j_k+j} - a_{j_k+j-1})}, & r_2 > t_{j_k+j}^{sup} > x^* \end{cases} \tag{46}$$

In order to guarantee that $t_{j_k+j}(l) \in [\delta_{j_k+j}, \min\left\{r_2, t_{j_k+j}^{sup}\right\}]$ when l ranging within the closed interval $[L_2^{\min}, L_2^{\max}]$ obtained above, the time instant $t_{j_k+j}(l)$ should be correspondingly set as

$$t_{j_k+j}(l) = \begin{cases} x_2 + t_{j_k+j-1}^b, & t_{j_k+j}^{sup} \geq r_2, \text{ or } x^* \leq t_{j_k+j}^{sup} \leq r_2 \text{ and } |\delta_{j_k+j} - x^*| \leq |t_{j_k+j}^{sup} - x^*| \\ x_1 + t_{j_k+j-1}^b, & t_{j_k+j}^{sup} \leq x^*, \text{ or } x^* \leq t_{j_k+j}^{sup} \leq r_2 \text{ and } |\delta_{j_k+j} - x^*| > |t_{j_k+j}^{sup} - x^*| \end{cases} \tag{47}$$

C. When considering the vehicle V_{j_k+j-1} has stopped

It can be easily seen that if the stopping time of the vehicle V_{j_k+j}, $t^b_{j_k+j}+\frac{-v_0}{a_{j_k+j}}$, were earlier than the stopping time of V_{j_k+j-1}, $t^s_{j_k+j-1}$, in this situation, no collision would occur. In this sense, $\overline{d}^{c3}_{j_k+j}$ can be simply set to 0. On the other side, if $t^s_{j_k+j-1} \leq t^b_{j_k+j}+\frac{-v_0}{a_{j_k+j}}$ and the initial inter-vehicular distance between V_{j_k+j-1} and V_{j_k+j} is given as l, the distance traveled by the vehicle V_{j_k+j} when it stops can be expressed as $dist_{j_k+j}(l)=\overline{d}_{j_k+j-1}+l$. Thus, substituting $dist_{j_k+j}(l)$ into (18) can yield $\overline{d}^{c3}_{j_k+j}=\frac{1}{p^{c3}_{j_k+j-1,j_k+j}}\int_{L_3^{\min}}^{L_3^{\max}}[\overline{d}_{j_k+j-1}+l]\rho e^{-\rho l}\mathrm{d}l$ where the parameters $L_3^{\min}$ and $L_3^{\max}$ are defined as the lower and upper bounds of l in the integral. Therefore, we can derive $\overline{d}^{c3}_{j_k+j}$ as

$$\overline{d}^{c3}_{j_k+j}=\frac{1}{p^{c3}_{j_k+j-1,j_k+j}}\times\begin{cases}0, & t^s_{j_k+j-1}>t^b_{j_k+j}+\dfrac{-v_0}{a_{j_k+j}}\\ \displaystyle\int_{L_3^{\min}}^{L_3^{\max}}[\overline{d}_{j_k+j-1}+l]\rho e^{-\rho l}\mathrm{d}l, & t^s_{j_k+j-1}\leq t^b_{j_k+j}+\dfrac{-v_0}{a_{j_k+j}}\end{cases}\tag{48}$$

In addition, if the rear vehicle V_{j_k+j} crashes into V_{j_k+j-1} which has stopped, it is required that $t^s_{j_k+j-1}\leq t^b_{j_k+j}-\frac{v_0}{a_{j_k+j}}$. Hence, a time instant $t_{j_k+j}(l)$ should exist and satisfy $t^s_{j_k+j-1}\leq t_{j_k+j}(l)\leq t^b_{j_k+j}-\frac{v_0}{a_{j_k+j}}$. Additionally, this rear-end collision could occur during V_{j_k+j} moving with the constant velocity v_0, or during V_{j_k+j} braking. In the first case, $t_{j_k+j}(l)$ is limited within $[t^s_{j_k+j-1},t^b_{j_k+j}]$, and we can get

$$v_0 t_{j_k+j}(l)=\overline{d}_{j_k+j-1}+l\tag{49}$$

In the second case, $t_{j_k+j}(l)$ satisfies $t^b_{j_k+j}<t_{j_k+j}(l)\leq t^b_{j_k+j}-\frac{v_0}{a_{j_k+j}}$, we get

$$v_0 t_{j_k+j}(l)+\frac{1}{2}a_{j_k+j}(t_{j_k+j}(l)-t^b_{j_k+j})^2=\overline{d}_{j_k+j-1}+l\tag{50}$$

Therefore, the upper bound $L_3^{\max}$ is obtained under the condition that V_{j_k+j} collides with V_{j_k+j-1} at the terminal time instant $t^b_{j_k+j}-\frac{v_0}{a_{j_k+j}}$ when V_{j_k+j} just happens to finish braking:

$$L_3^{\max}=v_0(t^b_{j_k+j}-\frac{v_0}{a_{j_k+j}})+\frac{1}{2}a_{j_k+j}(t^b_{j_k+j}-\frac{v_0}{a_{j_k+j}}-t^b_{j_k+j})^2-\overline{d}_{j_k+j-1}=v_0 t^b_{j_k+j}-\frac{v_0^2}{2a_{j_k+j}}-\overline{d}_{j_k+j-1}\tag{51}$$

But the lower bound $L_3^{\min}$ should be derived under the condition that V_{j_k+j} crashes into V_{j_k+j} before starting braking. That is,

$$L_3^{\min}=v_0 t^s_{j_k+j-1}-\overline{d}_{j_k+j-1}\tag{52}$$

.

3.3.2. Collision computation model if the rear vehicle is unequipped

The successive unequipped vehicle's movement are formulated with the car-following model defined by equation (8). From equation (10), it can be found that the velocity of an unequipped vehicle is a function of its own and its preceding vehicle. This means that there are no closed-form expressions for the velocity of an unequipped vehicle. Nevertheless, once the velocity of the preceding vehicle is updated, the velocity of this unequipped vehicle can be updated, subsequently. First, recalling equation (6), we rewrite the velocity of the equipped vehicle $V_{j_k+m_k}$ which is located in front of the first unequipped vehicle $V_{j_k+m_k+1}$ in the same subqueue as $v^*_{j_k+m_k}(t) = v_{j_k+m_k}(t) \times \left[1 - u(t - t^s_{j_k+m_k})\right]$. Subsequently, we can rearrange the equation (10) to recursively calculate the velocity of $V_{j_k+m_k+1}$ as:

$$v_{j_k+m_k+1}(t) = v_0 + \int_{\tau_{j_k+m_k+1}}^{t} \mu_{j_k+m_k+1} \times \left(v^*_{j_k+m_k}(l - \tau_{j_k+m_k+1}) - v_{j_k+m_k+1}(l - \tau_{j_k+m_k+1})\right) \mathrm{d}l \quad (53)$$

Additionally, we denote the time instant at which $V_{j_k+m_k+1}$ stops as $t^s_{j_k+m_k+1}$. Hence, the distance traveled by $V_{j_k+m_k+1}$ by the time t can be calculated by the integral as

$$d_{j_k+m_k+1}(t) = \begin{cases} \int_0^t \left(v_{j_k+m_k+1}(l)\right) \mathrm{d}l, & 0 \le t \le t^s_{j_k+m_k+1}; \\ \int_0^{t^s_{j_k+m_k+1}} \left(v_{j_k+m_k+1}(l)\right) \mathrm{d}l, & t > t^s_{j_k+m_k+1}. \end{cases} \quad (54)$$

The maximum distance traveled by $V_{j_k+m_k+1}$ should be attained when this vehicle can normally stop. That is, if the unequipped $V_{j_k+m_k+1}$ does not collide or be collided with others during braking in the car-following manner, its distance $d_{j_k+m_k+1}(t)$ will attain the maximum value at the time instant when $V_{j_k+m_k+1}$ stops. Let this maximum distance be $d^{max}_{j_k+m_k+1}$. Thus, we can set the value of $t^s_{j_k+m_k+1}$ equal to the time instant at which $v_{j_k+m_k+1}(t) = 0$, i.e., $v_{j_k+m_k+1}(t^s_{j_k+m_k+1}) = 0$, and then derive $d^{max}_{j_k+m_k+1} = d_{j_k+m_k+1}(t^s_{j_k+m_k+1})$. Therefore, similarly to the equation (15), the maximum relative distance between $V_{j_k+m_k}$ and $V_{j_k+m_k+1}$ can be approximated as

$$\Delta d^*_{j_k+m_k, j_k+m_k+1} = d^{max}_{j_k+m_k+1} - \overline{d}_{j_k+m_k} \quad (55)$$

And, based on the result of (55), the non-collision probability $p^{(1)}_{j_k+m_k, j_k+m_k+1}$ and collision probability $p^{(2)}_{j_k+m_k, j_k+m_k+1}$ can be calculated by (13) and (14).

After that, the actual value of the time instant $t^s_{j_k+m_k+1}$ should be recaclulated since $V_{j_k+m_k+1}$ may collide with its preceding vehicle or be collided by its rear vehicle before its traveled distance

attaining the maximum value. Once it is obtained, it is used to update the velocity of $V_{j_k+m_k+1}$ by using $v^*_{j_k+m_k+1}(t) = v_{j_k+m_k+1}(t) \times \Big[1 - u(t - t^s_{j_k+m_k+1})\Big]$. However, it is difficult to derive $t^s_{j_k+m_k+1}$ in the same approach to calculate the counterpart of an equipped vehicle by using (19). The reason is that the velocity of this unequipped vehicle $V_{j_k+m_k+1}$ are partially dependent on those of its preceding vehicle and it brakes in the car-following manner. It is not feasible to derive a closed-form expression to formulate the distance $dist_{j_k+m_k+1}(l)$ traveled by $V_{j_k+m_k+1}$ when given an initial inter-vehicular distance l. Consequently, nor is it feasible to calculate its expected distance $\overline{d}^c_{j_k+m_k+1}$ in the case of rear-end collision by equation (18), or to calculate the total expected distance $\overline{d}_{j_k+m_k+1}$ by equation (16). We derive this time instant $t^s_{j_k+m_k+1}$ by computing the expected relative distance $\Delta\overline{d}_{j_k+m_k,j_k+m_k+1}$ between $V_{j_k+m_k}$ and $V_{j_k+m_k+1}$. By referring to equation (16), $\Delta\overline{d}_{j_k+m_k,j_k+m_k+1}$ can be calculated as

$$\Delta\overline{d}_{j_k+m_k,j_k+m_k+1} = p^{(1)}_{j_k+m_k,j_k+m_k+1} \times \Delta\overline{d}^*_{j_k+m_k,j_k+m_k+1} + p^{(2)}_{j_k+m_k,j_k+m_k+1} \times \Delta\overline{d}^c_{j_k+m_k,j_k+m_k+1} \quad (56)$$

where $\Delta\overline{d}^c_{j_k+m_k,j_k+m_k+1}$ is the expected relative distance in the case of colliding with its preceding vehicle or being collided by its rear vehicle. By referring to equation (18), we derive the similar formula for computing $\Delta\overline{d}^c_{j_k+m_k,j_k+m_k+1}$: if an inter-vehicular distance is l, we can get

$$\begin{aligned}\Delta\overline{d}^c_{j_k+m_k,j_k+m_k+1} &= \frac{1}{p^{(2)}_{j_k+m_k,j_k+m_k+1}} \int_0^{\Delta\overline{d}^*_{j_k+m_k,j_k+m_k+1}} l\rho e^{-\rho l} \mathrm{d}l \\ &= \frac{1}{p^{(2)}_{j_k+m_k,j_k+m_k+1}} \left(\frac{1}{\rho} - \Delta\overline{d}^*_{j_k+m_k,j_k+m_k+1} e^{-\rho\Delta\overline{d}^*_{j_k+m_k,j_k+m_k+1}} - \frac{1}{\rho} e^{-\rho\Delta\overline{d}^*_{j_k+m_k,j_k+m_k+1}} \right)\end{aligned} \quad (57)$$

Once the expected distance $\Delta\overline{d}_{j_k+m_k,j_k+m_k+1}$ is calculated by the above equations, we can define a function as

$$W(t) = \Delta d_{j_k+m_k,j_k+m_k+1}(t) - \Delta\overline{d}_{j_k+m_k,j_k+m_k+1} = d_{j_k+m_k+1}(t) - d_{j_k+m_k}(t) - \Delta\overline{d}_{j_k+m_k,j_k+m_k+1} \quad (58)$$

Here, it should be noted that given a $\Delta\overline{d}_{j_k+m_k,j_k+m_k+1}$ obtained by the equation (56), at least one real root of $W(t) = 0$ exists. The proof is given in the following corollary:

Theorem 1 Given $\Delta\overline{d}_{j_k+m_k,j_k+m_k+1}$ and the corresponding $W(t)$ in (58), there exists at least one real root $\phi \in [0, +\infty)$ for the equation $W(t) = 0$

Proof 1 See Appendix Appendix A.■

Accordingly, we can set the time instant $t^s_{j_k+m_k+1}$ equal to the real root of the equation $W(t) = 0$, i.e., $W(t^s_{j_k+m_k+1}) = 0$, and use this time instant $t^s_{j_k+m_k+1}$ to update the velocity of $V_{j_k+m_k+1}$ as $v^*_{j_k+m_k+1}(t) = v_{j_k+m_k+1}(t) \times \left[1 - u(t - t^s_{j_k+m_k+1})\right]$. Moreover, we also set the expected distance $\overline{d}_{j_k+m_k+1}$ equal to the distance traveled by $V_{j_k+m_k+1}$ by the time instant $t^s_{j_k+m_k+1}$. That is, we can get $\overline{d}_{j_k+m_k+1} = d_{j_k+m_k+1}(t^s_{j_k+m_k+1})$. Once $\overline{d}_{j_k+m_k+1}$ is derived, the parameters $t^s_{j_k+m_k+i}$ and $\overline{d}_{j_k+m_k+i}$ of other rear unequipped vehicles $V_{j_k+m_k+i}$ $(i = 2, 3, \ldots, n_k)$ can also be computed by using the same procedure consisting of (53)∼(58). It is worth pointing out that in this computation framework, the computation of the velocity and distance of any unequipped vehicle should be recursive since they slow down in the car-following manner. The overall computation of those successive unequipped vehicles $\{V_{j_k+m_k+1}, V_{j_k+m_k+2}, \ldots, V_{j_k+m_k+n_k}\}$ can be summarized as the main four steps: initially, set $i = 1$ and then

Step 1: update the velocity $V_{j_k+m_k+i-1}$ by $v^*_{j_k+m_k+i-1}(t) = v_{j_k+m_k+i-1}(t) \times \left(1 - u\left(t - t^s_{j_k+m_k+i-1}\right)\right)$ and then recursively calculate $v_{j_k+m_k+i}(t)$ as well as $d_{j_k+m_k+i}(t)$ in this subqueue;

Step 2: calculate the maximum expected distance $d^{max}_{j_k+m_k+i}(t)$ as well as the maximum expected relative distance $\Delta d^*_{j_k+m_k+i-1,j_k+m_k+i}(t)$; based on these results, derive the non-collision and collision probabilities $p^{(1)}_{j_k+m_k+i-1,j_k+m_k+i}$ and $p^{(2)}_{j_k+m_k+i-1,j_k+m_k+i}$;

Step 3: calculate the expected relative distance in case of collision $\Delta\overline{d}^c_{j_k+m_k+i-1,j_k+m_k+i}$ as well as $\Delta\overline{d}_{j_k+m_k+i-1,j_k+m_k+i}$; then, solve the equation $W(t) = 0$ so as to get a real root ξ with these results. Thus, set $t^s_{j_k+m_k+i} = \xi$ and $\overline{d}_{j_k+m_k+i} = d_{j_k+m_k+i}(t^s_{j_k+m_k+i})$;

Step4 : if $i < n_k$, then set $i = i + 1$ and go to *Step 1* to continuously the procedure; otherwise, stop the procedure.

4. Computation of the average collision percentage

In this section, we firstly compute the vehicle collision times in the given subqueue, and then adopt the Monte Carlo based approach to derive the average collision percentage of the platoon based on the computation outcome of each subqueue. To achieve the computation of the average collision times in a subqueue, we adopt the Markov chain modeling technique used in [14], where the causal chain of possible rear-end collisions occurring between adjacent vehicles in a platoon is modeled as a probability tree diagram. To represent a stochastic state in the probability tree,

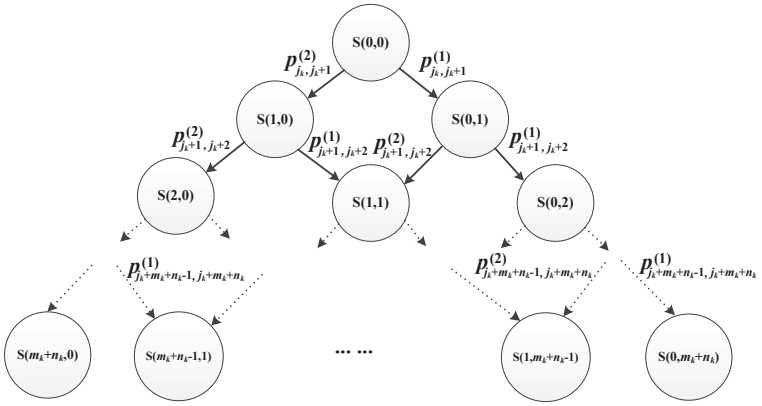

Figure 6 Probability tree diagram for a given subqueue.

we use the statistical concept of ''times'' as a measure of the frequency of an event occurring such as a rear-end collision or a successfully stopping instead of the amount of collided or successfully stopped vehicles. Hence, all the possible rear-end collision outcomes can be represented by the endings of the constructed probability tree.

4.1. Average collision percentage of a subqueue

When given a finite time window $[0, T]$, i.e., $t \in [0, T]$, based on the stochastic model proposed above, we can calculate the velocity, distance as well as the collision probability between any two adjacent vehicles in a given subqueue during $[0, T]$. Subsequently, we use the Markov chain to compute the average collision times occurring in the given subqueue. Here, we denote β_1 as the number of times of those vehicles in a given subqueue colliding with its preceding vehicle and β_2 as that of the vehicles successfully avoiding crashing into its preceding. Then, a probabilistic state can be defined as $S(\beta_1, \beta_2)$. Consider a given subqueue $\{V_{j_k}, \ldots, V_{j_k+m_k}, \ldots, V_{j_k+m_k+n_k}\}$ in which there exist $m_k + 1$ equipped vehicles and n_k unequipped vehicles. We can construct a probability tree for all possibilities of state transition of the given subqueue (see Fig. 6).

In Fig. 6, the initial state $S(0, 0)$ represents that only one equipped leading vehicle V_{j_k} exists and no collision occurs in this subqueue. Once a vehicle V_{j_k+1} comes to follow V_{j_k}, two possible events are considered to happen between V_{j_k+1} and V_{j_k}: i) V_{j_k+1} collides with V_{j_k}, or ii) V_{j_k+1} successfully avoids crashing into V_{j_k}. Accordingly, there are two possible states denoted by $S(1, 0)$ and $S(0, 1)$ to which the initial state $S(0, 0)$ will migrate. Similarly, when the next vehicle V_{j_k+2} follows V_{j_k+1}, each of the preceding states $S(1, 0)$ and $S(0, 1)$ is then possibly transferred to another two states, and so forth. The probability tree stretches until the last vehicle $V_{j_k+m_k+n_k}$ is considered. The

transition probability between any two possible states is defined as the non-collision probability $p^{(1)}_{j_k+i-1,j_k+i}$ or the collision probability $p^{(2)}_{j_k+i-1,j_k+i}$ $(i = 1, 2, \ldots, m_k + n_k)$. And these probabilities are calculated by the equations presented in Subsection 3.3.

From the probability tree in Fig. 6, we can see that there are totally $m_k + n_k + 1$ possible states at the end of the tree. One path from the initial state (the root of the probability tree) to one of the last states at the end of the tree structure (one leaf of the probability tree) represents one possible outcome of the given subqueue. And different paths may reach the same final outcome of the probability tree. Thus, in order to compute the probability of each outcome, we construct the transition probability matrix denoted by $\boldsymbol{P}$ so as to represent the transition relationships between the probabilistic states in the probability tree. There are totally $(m_k + n_k + 2) \times (m_k + n_k + 1)/2$ states in the Markov chain as $\{S(0,0), S(1,0), S(0,1), \ldots, S(0, m_k + n_k)\}$.

$$\boldsymbol{P} = \begin{bmatrix}
0 & p^{(2)}_{j_k,j_k+1} & p^{(1)}_{j_k,j_k+1} & 0 & 0 & 0 & 0 & 0 & 0 & 0 & \ldots & 0 \\
0 & 0 & 0 & p^{(2)}_{j_k+1,j_k+2} & p^{(1)}_{j_k+1,j_k+2} & 0 & 0 & 0 & 0 & 0 & \ldots & 0 \\
0 & 0 & 0 & 0 & p^{(2)}_{j_k+1,j_k+2} & p^{(1)}_{j_k+1,j_k+2} & 0 & 0 & 0 & 0 & \ldots & 0 \\
0 & 0 & 0 & 0 & 0 & 0 & p^{(2)}_{j_k+2,j_k+3} & p^{(1)}_{j_k+2,j_k+3} & 0 & 0 & \ldots & 0 \\
0 & 0 & 0 & 0 & 0 & 0 & 0 & p^{(2)}_{j_k+2,j_k+3} & p^{(1)}_{j_k+2,j_k+3} & 0 & \ldots & 0 \\
0 & 0 & 0 & 0 & 0 & 0 & 0 & 0 & p^{(2)}_{j_k+2,j_k+3} & p^{(1)}_{j_k+2,j_k+3} & \ldots & 0 \\
\vdots & \vdots & \vdots & \vdots & \vdots & \vdots & \vdots & \vdots & \vdots & \vdots & \ddots & \vdots \\
0 & 0 & 0 & 0 & 0 & 0 & 0 & 0 & 0 & 0 & \ldots & 0
\end{bmatrix} \tag{59}$$

Each element in the first row of $\boldsymbol{P}$ corresponds to the probability of the initial state transferring to each state in the Markov chain by one step. The Markov chain is homogeneous so that the probabilities of the initial state reaching each of $m_k + n_k + 1$ final states by taking $m_k + n_k$ steps can be given by the last $m_k + n_k + 1$ elements in the first row of $\boldsymbol{P}^{m_k+n_k}$. Given that the element at the o_1th row and the o_2th column of $\boldsymbol{P}^{m_k+n_k}$ can be indexed as $\boldsymbol{P}^{m_k+n_k}[o_1, o_2]$, and the probability of q collision events occurring in the given subqueue is denoted as $p_q(m_k, n_k)$ $(q = 0, 1, \ldots, m_k + n_k)$. Then, we have

$$p_q(m_k, n_k) = \boldsymbol{P}^{m_k+n_k}[1, \frac{(m_k + n_k + 2)(m_k + n_k + 1)}{2} - q] \tag{60}$$

Therefore, following (60), we can compute the expected number of times of vehicle collision in this given subqueue, i.e. the average vehicle collision times, as follows:

$$N^c(m_k, n_k) = \sum_{q=0}^{m_k+n_k} q \times p_q(m_k, n_k) \tag{61}$$

In addition, we also can compute the average collision percentage of the given subqueue by determining the ratio between the number of times of collision events and the total amount of events. Let P_c^k be the average collision percentage. We obtain the value of P_c^k by

$$P_c^k = \frac{N^c(m_k, n_k)}{m_k + n_k} \tag{62}$$

In order to validate the equations proposed in Subsections 3.3 and 4.1, we conduct a numerical experiment in which we compare the result of the proposed stochastic model with that of Monte Carlo simulation. In the given subqueue, the total number of vehicles is set to 10 and the penetration rate of the equipped vehicle is set to 0.4. That is, the amount of the equipped vehicles is $4 = 0.4 \times 10$. The four equipped vehicles are located in front of those successive 6 unequipped vehicles. And Their initial velocity is set to 90km/h. Furthermore, the deceleration of those equipped vehicles are set different from each other's. Without loss of generality, their decelerations are assumed to be generated from the uniform distribution between -7.5 and -4.5 m/s^2, and the maximum deceleration of all the unequipped vehicles is limited to -8 m/s^2. Now, we come to consider these timing parameters δ_j (since there are 4 equipped vehicles in this subqueue, so $j = 1, 2, 3, 4$) and τ_i (for $i = 5, \ldots, 10$). By referring to the DSRC-based transmission and broadcasting latencies discussed in [22], the transmission latency $\gamma_j^{(1)}$ can be $0 \sim 25$ ms in normal condition while the broadcasting latency $\gamma_j^{(2)}$ can be $100 \sim 1000$ ms. In the experiment, we fix each $\gamma_j^{(1)}$ as 20 ms and uniformly stochastically generate $\gamma_j^{(2)}$ in $[100, 1000]$ ms. The vehicular braking system reaction time to generate the expected deceleration from a stimulus on the brake pedal ε_i should not be neglected. This vehicle reaction time is dependent on the comprehensive dynamic performance of the vehicle V_i. Its precise estimation is complex and out of the scope of this work. For the sake of example, every ε_i $(i = 1, 2 \ldots, 10)$ is generated from the uniform distribution between 30 and 70 ms. As discussed in [22, 31–34], the driver reaction time depends on several complex factors such as driver's age, brake reaction time and neural central processing time, etc. Its test value usually varies around 500 ms in those works. In our experiment, we simply set the driver reaction time ϵ_j as a uniform random variable between 400 and 1000 ms for the equipped vehicles V_j $(j = 1, 2, 3, 4)$. And as for the unequipped vehicles V_i $(i = 5, \ldots, 10)$, we uniformly and stochastically set the sum of the driver perception and reaction times $(\kappa_i + \epsilon_i)$ which is between $2.5 - 0.3 = 2.2$s and $2.5 + 0.3 = 2.8$s according to the suggestion from [22, 35]. In the experiment, the average initial inter-vehicular distance is $1/\rho - L$ and it is set to discretely range from $(5 - L)$m to $(150 - L)$m.

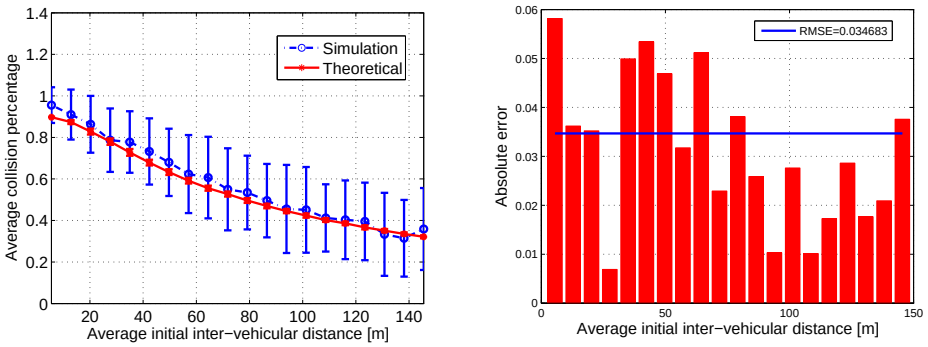

(a) The average collision percentage. (b) The absolute errors.

Figure 7 Validation of the computation model when given a subqueue.

The length of every vehicle is set $L = 4.5$m. Thus, each initial inter-vehicular distance between vehicles can be independently stochastically generated by following the exponential distribution with the parameter ρ. Additionally, both of the theoretical model-based computation and the comparative Monte Carlo simulation are repeatedly performed 100 times at each point of the initial inter-vehicular distance so that the corresponding averaged result and its standard deviation can be derived for comparison. The experimental results are shown in Fig.7. From Fig.7(a), it can be found that the results obtained by our proposed computation model well approximates those of simulation. In Fig.7(b), the root mean squared error between the theoretical and simulated results is about 3.5%. At this point, it proves that it is reasonable enough to use the mathematical expectation of the distance traveled by each individual vehicle and the expected relative inter-vehicular distance to formulate the computation model when taking into account the stochastic nature of inter-vehicular distance distribution. And the Markov Chain model represented as the tree-type diagram is also validated by those comparative results.

4.2. Average collision percentage of the platoon

As mentioned before, we have divided the overall vehicle platoon $\mathbb{V}$ ($|\mathbb{V}| = N$) into $M+1$ subqueues. Recalling that in the k^{th} subqueue the total number of vehicles is $1+m_k+n_k$, we can get $N+1 = \sum_{k=0}^{M}(1+m_k+n_k)$ and the total amount of the equipped vehicles is $C = \sum_{k=0}^{M}(m_k+1)$. When considering the actual scenario where those equipped vehicles are stochastically distributed in the platoon and the vehicle amount is large, the number of the approaches to divide the platoon will be tremendously large. That is, if the penetration rate of the equipped vehicles (we denote thise

penetration rate as α) and the total amount of the vehicles $(N+1)$ are given, the number of the subqueues $M+1$, the number of the equipped vehicles m_k+1 and the unequipped vehicle amount n_k in each subqueue have large amounts of possible values. It is not feasible to enumerate all the possible situations. Therefore, we adopt the Monte Carlo simulation approach to approximate the stochastic distribution of those equipped vehicles in the given platoon.

Let the number of times of performing Monte Carlo simulation be an appropriate finite integer $SimNum$ ($SimNum > 0$). In each Monte Carlo simulation, let the leading vehicle of the platoon be an equipped one. Additionally, we stochastically assign $\lfloor \alpha \times (N+1) \rfloor$ vehicles of the platoon as the equipped vehicles. Subsequently, the given platoon can be divided into a series of subqueues according to the distribution of those equipped vehicles generated by Monte Carlo simulation. Thus, the numbers of those equipped and unequipped vehicles in each subqueue can also be determined respectively. Let Q_v be the set of the results of dividing the whole platoon through stochastically assigning those equipped vehicles in the v^{th} Monte Carlo simulation. For simplicity, this set Q_v is expressed as

$$Q_v = \{(m_k^v, n_k^v) | m_k^v \text{ and } n_k^v \geq 0 \text{ for } k = 0, 1, \ldots, M^v\} \tag{63}$$

where (M^v+1) is the total number of the subqueues determined in the v^{th} Monte Carlo simulation, (m_k^v+1) and n_k^v are the equipped and the unequipped vehicle amounts in the k^{th} subqueue in this simulation. And these parameters should satisfy that $N+1 = \sum_{k=0}^{M^v}(1+m_k^v+n_k^v)$ and $\lfloor \alpha \times (N+1) \rfloor = \sum_{0}^{M^v}(1+m_k^v)$. Furthermore, based on the equation (61), we can approximate the total expected number of rear-end collision events occurring in the platoon when considering that those equipped vehicles are stochastically distributed as follows:

$$\overline{N}^c = \frac{\sum_{v=1}^{SimNum} \sum_{(m_k,n_k)\in Q_v} N^c(m_k, n_k)}{SimNum} = \frac{\sum_{v=1}^{SimNum} \sum_{(m_k,n_k)\in Q_v} \sum_{q=0}^{m_k+n_k} q \times p_q(m_k, n_k)}{SimNum} \tag{64}$$

By following (64), the average collision percentage of the whole platoon can be denoted as P^c and calculated as

$$P^c = \frac{\overline{N}^c}{N} \tag{65}$$

5. Experiments

In this section, the validation as well as the application of the proposed stochastic model is investigated through extensive numerical experiments. To comparatively validate the results obtained by our computation model, we also conduct extensive Monte Carlo simulations and perform

the comparison between the results of the theoretical computations and the simulations. Different traffic scenarios are set up to demonstrate the utilization of the model. All the numerical experiments including the theoretical computations and Monte Carlo simulations are implemented in MATLAB.

5.1. Model validations

We simulate two traffic scenarios for the model validation. In these two simulated scenarios, the total amount of vehicles in the platoon is fixed at $(N+1) = 25$. The length of each vehicle is fixed at 4.5m. The average initial inter-vehicular distance $(1/\rho - L)$ discretely ranges from 10-L=5.5m to 150-L=145.5m. And we assume that at the initial time instant $t_0 = 0$ the leader of the given platoon starts braking. On the other side, we vary the penetration rate of the equipped vehicles in the platoon as $\alpha \in \{0.1, 0.3, 0.5, 0.7, 0.9\}$, so as to compare the numerical results obtained by our theoretical model and by the Monte Carlo simulations over those different penetration rates. Furthermore, in each of these two traffic scenarios, we conduct three cases so as to validate our theoretical model with different parameter settings. The basic characteristics of each of the simulation cases in each of the two mobility scenarios are summarized in Tab.I. Those significant parameters involved in the proposed computation model include the driver sensitivity coefficient μ_i in the car-following model, the timing parameters τ_i and δ_j. The details on different parameter settings are described as follows:

Table I The characteristics of different simulation cases.

settings	scenarios
	high mobility: $v_0 = 110$km/h & low mobility: $v_0 = 60$km/h
Case 1	$\mu_i \sim U(0.6, 1)\text{s}^{-1}$, $a_j \sim U(-7.5, -4.5)\text{m/s}^2$.
Case 2	$(\kappa_i + \epsilon_i) \sim U(2.2, 2.8)$s, $\gamma_j^{(2)} \sim U(100, 1000)$ms
Case 3	$\mu_i, (\kappa_i + \epsilon_i), a_j, \gamma_j^{(2)}$ set as in Case 1 and Case 2, $\epsilon_j \sim U(300, 700)$ms

i) In the first case, we simply fix the driver perception and reaction time $(\kappa_i + \epsilon_i)$ at 2.5s for every unequipped vehicle and the vehicle deceleration time ε_i at 50ms for all the vehicles. Also, the reaction time of those equipped vehicle driver ϵ_j is set at 0.5s. As for those equipped vehicles, their DSRC-based transmission latency $\gamma_j^{(1)}$ and broadcasting latency $\gamma_j^{(2)}$ are fixed at 25ms and 100ms.

On the other side, we vary the driver sensitivity coefficient μ_i for each unequipped vehicle and the deceleration a_j for each equipped vehicle in this case. Here, those μ_i are assumed to identically and independently follow a uniform distribution whose limited interval is set as $[0.6, 1]\text{s}^{-1}$.

ii) We consider to vary $(\kappa_i + \epsilon_i)$ and $\gamma_j^{(2)}$ in the second case. Here, $(\kappa_i + \epsilon_i)$ and $\gamma_j^{(2)}$ are also assumed to be random variables following the uniform stochastic distribution. Besides, in this case, μ_i is fixed at 0.8s^{-1} for all the unequipped vehicles, and the deceleration a_j at -6m/s^2 for all the equipped vehicles. The other parameter settings in the second case are the same as those of the first case.

iii) In the third case, the vehicle deceleration time ε_i is fixed at 50ms for all the vehicles and the transmission latency $\gamma_j^{(1)}$ at 25ms for those equipped vehicles. In addition, the parameters related to the unequipped vehicles $(\kappa_i + \epsilon_i), \mu_i$ (for $\forall\ V_i \in \mathbb{V}_U$), and those related to the equipped vehicles $\epsilon_j, \gamma_j^{(2)}, a_j$ (for $\forall\ V_j \in \mathbb{V}_E$) are assumed to be uniform random variables.

In the Monte Carlo simulation, the initial space headway between vehicles is stochastically generated from the exponential distribution with ρ. And the motion of each unequipped vehicle is simulated in the car-following behavior while those equipped can independently decelerate (see Subsection 3.2). The Monte Carlo simulation is performed with 100 replications at each point of $(1/\rho - L)$, and the simulation outcomes are then averaged. It is worth pointing out that at each point of $(1/\rho - L)$ we also compute the proposed theoretical model with 100 replications and provide the average value of its outcomes, since we adopt the Monte Carlo simulation based technique to approximate the stochastic distribution of those equipped vehicles in the platoon. In the following figures of this subsection, the theoretical computing results are presented by the solid line while those results obtained by the simulations are marked by the dashed line. All the results corresponding to different penetration rate settings are represented in different colors: the results obtained with $\alpha = 0.1$ are colored in red, those with $\alpha = 0.3$, $\alpha = 0.5$, $\alpha = 0.7$ and $\alpha = 0.9$ are assigned in blue, green, magenta and cyan, respectively. Besides, the standard deviation of the results at each point is represented by the error bar.

5.1.1. High mobility scenario

In the first scenario, the initial velocity v_0 of all vehicles in the platoon is identically set to a relatively high value, i.e. $v_0 = 110\text{km/h}$. The results obtained by computing our stochastic model and by processing Monte Carlo simulation are shown in Fig. 8. It can be found that when

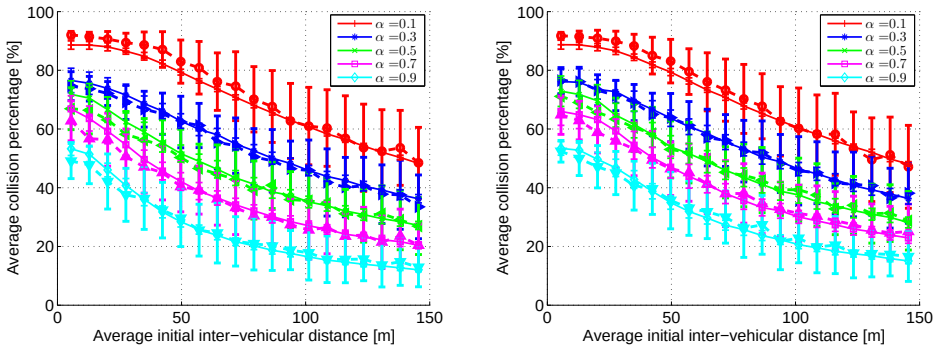

(a) Case 1 (b) Case 2

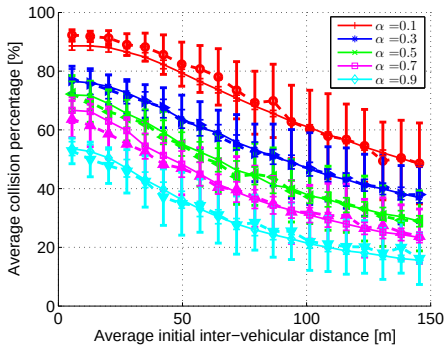

(c) Case 3

Figure 8 The model validation in the high mobility scenario.

the average inter-vehicular distance is small and the penetration rate α of the equipped vehicles is low, the value of average collision percentage is relatively higher. For example, the average collision percentages at the data point of $(1/\rho - L) = 5.5$m with $\alpha = 0.1$ are above 90%. However, the probability of chain collisions in the platoon is relatively smaller, when both $(1/\rho - L)$ and α are large enough. The reason is that the larger inter-vehicular distance is reserved for vehicle's deceleration, the smaller the chance of vehicle crashing into its preceding one becomes, and the more vehicles are equipped with inter-vehicular communications, the shorter the cumulative arrival time of warning message propagating between vehicles is. Moreover, those subfigures show that the theoretical results are close to those of the simulations. At this point, our theoretical model can capture the basic property of the platoon as the simulation based approach does.

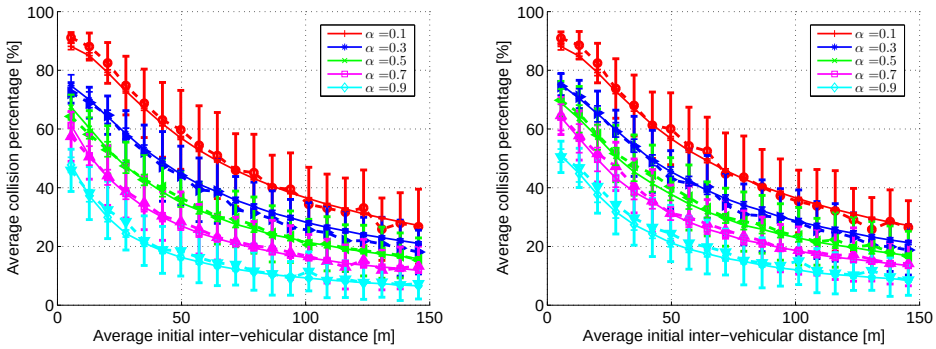

(a) Case 1

(b) Case 2

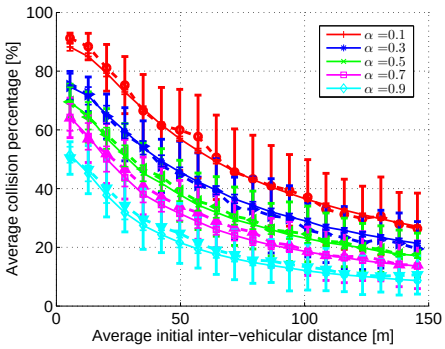

(c) Case 3

Figure 9 The model validation in the low mobility scenario.

5.1.2. Low mobility scenario

Different from the high mobility scenario, in the low mobility scenario, the initial velocity is set as $v_0 = 60$km/h. And the results are illustrated in Fig. 9. The similar conclusion can also be drawn. It can be seen that our stochastic model provides an excellent approximation to the exact outcomes from the simulations. Moreover, it can be found that the lower mobility may lead to less rear-end collision in the given platoon under the same penetration rate. For example, when the average initial inter-vehicular distance is set to about 100m and $\alpha = 0.9$, the average collision percentages obtained in the three cases of the high mobility scenario are around 20%, while those obtained in the low mobility are obviously below 20%. The results is consistent with the fact that the relatively smaller velocity could result in a lower severity of vehicular rear-end collision when compared to the high mobility situation in the same traffic density. In both scenarios, the results of the theoretical model well approximates those of simulations and capture the actual fact.

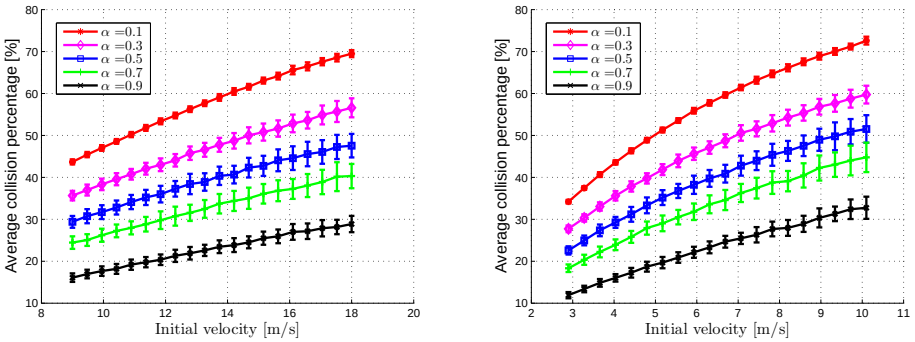

(a) Non-peak-hour (b) Peak-hour

Figure 10 The average collision percentage in two scenarios with different mean velocities.

5.2. Model applications

To show the model applications, we conduct the following experiments. We set up two typical traffic urban scenarios: one is related to the urban traffic flow during the peak hours and another is the non-peak hour traffic flow. Generally, the space headway distribution and the mean velocity of the traffic flow are two main parameters to characterize these two traffic scenarios. Thus, we focus on different settings of those two parameters. In the following experiments, we also assume that all the vehicles have the same length $L = 4.5$m. In the peak-hour traffic scenario, the average space headway between vehicles is set as $1/\rho = 18$m. That is, in this scenario, the average initial inter-vehicular distance is set to $(1/\rho - L) = 18 - 4.5 = 13.5$m. And the mean velocity of the traffic flow is set to 6.5m/s. For comparison, the average space headway is fixed at 40m in the non-peak-hour scenario (similarly, the average initial inter-vehicular distance is equal to $40 - 4.5 = 35.5$m in this scenario). In addition, the mean traffic flow velocity is set to a relatively high value 13.5m/s. For both scenarios, the number of the vehicles in the platoon is also equal to $(N + 1) = 25$. Hence, with those parameter settings corresponding to the different traffic scenarios, we are allowed to apply our proposed model to evaluate the influence of the different model parameters on the chain collision in a given platoon.

5.2.1. Evaluation of the influence of the different initial velocities on the average collision percentage

Fig. 10 shows the results with different settings on the initial velocity of the platoon as well as on the penetration rate α. The initial velocity v_0 ranges within different intervals in the two traffic

scenarios. In the non-peak-hour traffic scenario, v_0 discretely ranges within $[13.5 - 3 \times 1.5, 13.5 + 3 \times 1.5] = [9, 18]$ m/s, while in the peak-hour traffic scenario within $[6.5 - 3 \times 1.2, 6.5 + 3 \times 1.2] = [2.9, 10.1]$ m/s. The other parameters are set in the same way of the third case in the previous experiments for model validation: the vehicle deceleration time ε_i is fixed at 50ms for every vehicle, the transmission latency $\gamma_j^{(1)}$ at 25ms for those equipped vehicles, while $(\kappa_i + \epsilon_i) \sim U(2.2, 2.8)$s, $\mu_i \sim U(0.6, 1)\text{s}^{-1}$, $\epsilon_j \sim U(300, 700)$ms, $\gamma_j^{(2)} \sim U(100, 1000)$ms, $a_j \sim U(-7.5, -4.5)\text{m/s}^2$. It should be pointed out that at each point of the initial velocity the theoretical model is performed with 100 replications and then, the averaged result and its corresponding standard deviation at each point are provided in the following figures (illustrated by markers and error bars, respectively).

From Fig. 10, it can be found that the slope of the curve corresponding to a smaller α is relatively larger. That is, when the penetration rate of those equipped vehicles in the given platoon is relatively smaller (e.g., when the penetration rate α is set to be 0.1), the average collision percentage is more sensitive to the variability of the initial velocity. But a relatively larger penetration rate can reduce that sensitivity so as to make the variation of the average collision percentage over the velocity become gentler. Furthermore, by comparing Fig. 10(a) and Fig. 10(b), it can be found that when given the same initial velocity (e.g., $v_0 = 9$m/s) and attempting to guarantee the same degree of average collision percentage (e.g., $P^c = 30\%$) in the two scenarios, the penetration rate α needs to be 0.5 in the non-peak-hour scenario while α should be set to 0.9 in the peak-hour scenario. The reason is that the inter-vehicular distance in the peak-hour scenario is much smaller on average than that in the non-peak-hour scenario. Nevertheless, from another perspective, this also implies that with the same velocity and safety level, a larger penetration rate of the equipped vehicles can improve the capacity of the road. That is, when more vehicles are equipped with inter-vehicular communications, the inter-vehicular distance can be appropriately reduced in a general traffic flow at the meanwhile maintaining a certain safety level of the traffic flow. No matter what traffic scenarios the vehicle platoon moves in, the increase in the penetration rate of the equipped vehicles in the platoon will lead to the decrease in the average collision percentage. The fact indicated by the experiment results is reasonable and consistent with the researches of [9, 26].

5.2.2. Evaluation of the influence of the different driver perception and reaction times on the average collision percentage

In the next experiment, we fix the parameter v_0 at the mean velocity of both scenarios, i.e., $v_0 = 13.5$m/s in the non-peak-hour traffic scenario and $v_0 = 6.5$m/s in the peak-hour traffic scenario. The driver perception and reaction time $(\kappa_i + \epsilon_i)$ $(\forall V_i \in \mathbb{V}_U)$ is set to range within $[2.2, 2.8]$s, and the penetration rate $\alpha \in \{0.1, 0.3, 0.5, 0.7, 0.9\}$ for both scenarios. Meanwhile, the other parameters are set as: $\varepsilon_i = 50$ms (for $\forall V_i \in \mathbb{V}$), $\gamma_j^{(1)} = 25$ms (for $\forall V_j \in \mathbb{V}_E$), $\gamma_j^{(2)} = 100$ms (for $\forall V_j \in \mathbb{V}_E$), $\mu_i = 0.8\text{s}^{-1}$ (for $\forall V_i \in \mathbb{V}_U$), $\epsilon_j = 500$ms (for $\forall V_j \in \mathbb{V}_E$) and $a_j \sim U(-7.5, -4.5)\text{m/s}^2$ (for $\forall V_j \in \mathbb{V}_E$).

The numerical results of evaluating the impact of the parameter $(\kappa_i + \epsilon_i)$ combined with α are given in Fig.11. From these results, we can see that a larger latency of the manual operation could lead to a higher severity of the rear-end collision in both traffic scenarios. However, the safety degree of the platoon can be improved by increasing the penetration rate of the equipped vehicles. For instance, in both scenarios, when α increases to 0.9, the average collision percentage is maintained under 20%. From these figures, it can be found that a slight increase in the penetration rate could result in a obvious decrease in the average collision percentage. This confirms the improvement of traffic safety induced by inter-vehicular communications. On the other hand, the statistical difference between the results in the non-peak-hour and the peak-hour scenarios is moderate when α is set to the same value. The reason is that the potential of the rear-end collision is not only dependent on the inter-vehicular distance but also the vehicular velocity. That is, even though the inter-vehicular distance is smaller in the peak-hour scenario when compared to that in the non-peak-hour scenario, the mean traffic velocity is also relatively smaller. So, it does not seem to be an obvious difference between the potentials of the rear-end collision in these traffic scenarios when the penetration rates of these scenarios are the same value.

5.2.3. Evaluation of the influence of the different broadcasting latencies on the average collision percentage

Generally, the broadcasting frequency of different vehicular communication system may differ, and the magnitude of the broadcasting latency could range in a certain larger interval when compared to the transmission latency that is mainly dependent on the process of the physical communication. Thus, similarly to the experiment in the 5.2.2, we investigate the impact of the parameter

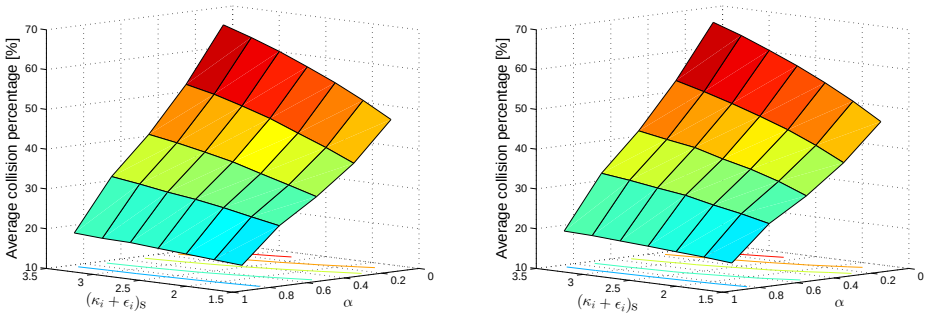

(a) Non-peak-hour (b) Peak-hour

Figure 11 The average collision percentage in two scenarios with different settings on $(\kappa_i+\epsilon_i)$ (for $\forall V_i \in \mathbb{V}_U$) and α.

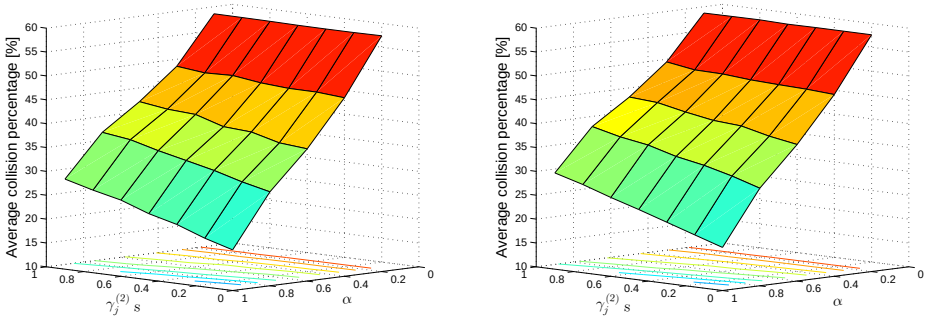

(a) Non-peak-hour (b) Peak-hour

Figure 12 The average collision percentage in two scenarios with different settings on $\gamma_j^{(2)}$ (for $\forall V_j \in \mathbb{V}_E$) and α.

$\gamma_j^{(2)}$ (for $\forall V_j \in \mathbb{V}_E$) on the potential of chain collisions in the platoon. By referring to [22], we vary $\gamma_j^{(2)}$ from 100ms to 1000ms. The penetration rate is also set as $\alpha \in \{0.1, 0.3, 0.5, 0.7, 0.9\}$. Except that the parameter related to the driver perception and reaction time of those unequipped vehicles $(\kappa_i + \epsilon_i)$ is fixed at 2.5s for $\forall V_i \in \mathbb{V}_U$, the settings on the other parameters including v_0, ε_i (for $\forall V_i \in \mathbb{V}$), $\gamma_j^{(1)}$ (for $\forall V_j \in \mathbb{V}_E$), μ_i (for $\forall V_i \in \mathbb{V}_U$), ϵ_j (for $\forall V_j \in \mathbb{V}_E$) and a_j (for $\forall V_j \in \mathbb{V}_E$) are the same as those in the experiment of the 5.2.2.

The similar conclusion can also be drawn from the experimental results given in Fig.12. A larger warning information propagation latency between those equipped vehicles could induce a higher average collision percentage. On the other side, from Fig.12, it can be found that when α

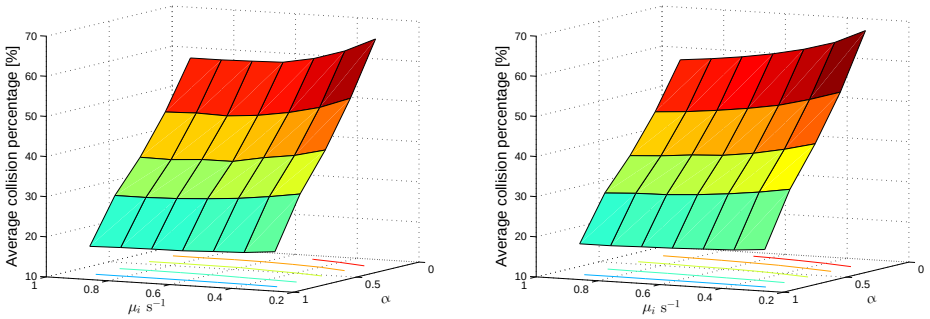

(a) Non-peak-hour (b) Peak-hour

Figure 13 The average collision percentage in two scenarios with different settings on μ_i (for $\forall V_i \in \mathbb{V}_U$) and α.

is set to be a relatively higher value (e.g., $\alpha = 0.9$), the average collision percentage does seem to be more sensitive to the variation of $\gamma_j^{(2)}$. That is, with $\alpha = 0.9$, the average collision percentage will decrease more abruptly along with decreasing $\gamma_j^{(2)}$ when compared to other situations where α is set to a relatively smaller value such as 0.5, 0.3 or 0.1, etc. This result suggests that the performance of the inter-vehicular communication system indicated by the message broadcasting delay really has a remarkable impact on the potential of chain collisions in the overall platoon, and vehicles can benefit from a more reliable and low-latency vehicular communication system, especially when the penetration rate is high.

5.2.4. Evaluation of the influence of the different driver sensitivity coefficients on the average collision percentage

Since μ_i is an important parameter to indicate the driver sensitivity of those unequipped vehicles, in the final experiment, we use our proposed model to evaluate the influence of μ_i on the chain collisions in the platoon. Here, we consider that μ_i for $(\forall V_i \in \mathbb{V}_U)$ ranges within $[0.3, 0.9]$ s^{-1} and α is also set as $\alpha \in \{0.1, 0.3, 0.5, 0.7, 0.9\}$. Similarly to the 5.2.3, let $(\kappa_i + \epsilon_i)$ equal to 2.5s. Also, we set $\gamma_j^{(2)} = 100$ms for $\forall V_j \in \mathbb{V}_E$. The settings on the other parameters such as v_0, ε_i (for $\forall V_i \in \mathbb{V}$), $\gamma_j^{(1)}$ (for $\forall V_j \in \mathbb{V}_E$), ϵ_j (for $\forall V_j \in \mathbb{V}_E$) and a_j (for $\forall V_j \in \mathbb{V}_E$) are the same as those in the 5.2.2.

The results are shown in Fig.13. It can be found that the average collision percentage is sensitive to the driver's sensitivity coefficient, especially when the penetration rate is kept at a low level (e.g. $\alpha = 0.1$). In both traffic scenarios, the larger the parameter μ_i is, the lower the accident severity

becomes. This result is consistent with the fact that a driver with a higher sensitivity will push on the brake pedal more sharply so as to generate a larger deceleration for collision avoidance. On the other hand, the increase in the penetration rate can reduce the variability of the average collision percentage resulting from the variation of μ_i. That is, even with a relatively lower sensitivity, a higher penetration rate could make up the shortage due to the low driver sensitivity. For example, when α attains 0.9, the average collision percentage can be maintained below 20% regardless of μ_i ranging from 0.3s^{-1} to 0.9s^{-1}. This strengthens once more that the overall safety degree of the platoon can be enhanced by inter-vehicular communications.

6. Conclusions

In this paper we propose a computation model for analyzing the process of collisions potentially occurring in a platoon, where considering only partial vehicles are equipped with inter-vehicular communications. The model supports the scenarios where the DSRC equipped vehicles are stochastically distributed, and the inter-vehicular distance between adjacent vehicles follows a certain stochastic distribution. Furthermore, the model is independent of the driver-related operation characteristics and the vehicle-related reaction latency, so it enables the safety evaluation of different driver characteristics and vehicle brake control system in the different traffic scenarios. The usability and accuracy of this model is tested and validated by comparing its theoretical computing results with those of extensive Monte Carlo simulations under different parameter settings. Based on the proposed model, we have also presented extensive experiments in different traffic scenarios to analyze the influence of DSRC penetration rates, inter-vehicular broadcasting latency, driver reaction latency and vehicular kinematic characteristics on the potential of the rear-end collision occurring in the platoon. As model application, it can be drawn from the numerical evaluation results of our proposed model that the increased inter-vehicular distance and the penetration rate can alleviate chain collisions in the platoon. Another conclusion can also be indicated from those numerical results provided by our model that even with a part of equipped vehicles, it is possible to keep the severity of chain collisions in the platoon below a certain level when some driver, vehicle, inter-vehicular communication system related characteristics are appropriately constrained such as the driver perception and reaction time, the driver sensitivity, the vehicle speed and the broadcasting latency.

Acknowledgements

This research was supported, in part, by the National Natural Science Foundation of China under Grant nos. U1564212, 61103098 and 91118008.

Appendix A. Proof of Theorem 1

First, we introduce an inequality as follows. It can be proven that for all $x \in (0, +\infty)$,

$$x \geq 1 - e^{-x}. \tag{A.1}$$

Next, let $x = \rho\Delta d^*$, and substitute this x into (A.1). Subsequently, we can get

$$\begin{aligned}
&\rho\Delta d^* \geq 1 - e^{-\rho\Delta d^*} \\
&\Delta d^* \geq \frac{1}{\rho} - \frac{1}{\rho}e^{-\rho\Delta d^*} \\
&\Delta d^* \left(1 - e^{-\rho\Delta d^*}\right) \geq \frac{1}{\rho} - \Delta d^* e^{-\rho\Delta d^*} - \frac{1}{\rho}e^{-\rho\Delta d^*} \\
&\Delta d^* \geq \frac{\left(\frac{1}{\rho} - \Delta d^* e^{-\rho\Delta d^*} - \frac{1}{\rho}e^{-\rho\Delta d^*}\right)}{1 - e^{-\rho\Delta d^*}}
\end{aligned} \tag{A.2}$$

where we use Δd^* to denote $\Delta d^*_{j_k+m_k,j_k+m_k+1}$ for the sake of simplicity.

Accordingly, by the expressions of $p^{(2)}_{j_k+m_k,j_k+m_k+1}$ and $\Delta d^c_{j_k+m_k,j_k+m_k+1}$, it can be observed that

$$\Delta d^*_{j_k+m_k,j_k+m_k+1} \geq \Delta d^c_{j_k+m_k,j_k+m_k+1} \tag{A.3}$$

Note that $t \in (0, +\infty)$. Hence, by setting $t = 0$, we can observe $d_{j_k+m_k+1}(0) = d_{j_k+m_k+1}(0)$ and

$$W(0) = d_{j_k+m_k+1}(0) - d_{j_k+m_k,j_k+m_k+1}(0) - \Delta\overline{d}_{j_k+m_k+1} = -\Delta\overline{d}_{j_k+m_k+1} < 0 \tag{A.4}$$

On the other hand, within the open interval $(0, +\infty)$, there must be at least one time instant that makes the term $(d_{j_k+m_k+1}(t) - d_{j_k+m_k,j_k+m_k+1}(t))$ attain the maximum value $\Delta d^*_{j_k+m_k,j_k+m_k+1}$. We denote this time instant as ϕ. That is, we have

$$(d_{j_k+m_k+1}(\phi) - d_{j_k+m_k,j_k+m_k+1}(\phi)) = \Delta d^*_{j_k+m_k,j_k+m_k+1} \tag{A.5}$$

Hence, according to (56) and (A.3), we can further get

$$\begin{aligned} W(\phi) &= \Delta d^{*}_{j_k+m_k,j_k+m_k+1} - \Delta \overline{d}_{j_k+m_k,j_k+m_k+1} \\ &= \Delta d^{*}_{j_k+m_k,j_k+m_k+1} - \left(p^{(1)}_{j_k+m_k,j_k+m_k+1} \times \Delta \overline{d}^{*}_{j_k+m_k,j_k+m_k+1} + p^{(2)}_{j_k+m_k,j_k+m_k+1} \times \Delta \overline{d}^{c}_{j_k+m_k,j_k+m_k+1} \right) \\ &\geq \Delta d^{*}_{j_k+m_k,j_k+m_k+1} - \left(p^{(1)}_{j_k+m_k,j_k+m_k+1} \times \Delta \overline{d}^{*}_{j_k+m_k,j_k+m_k+1} + p^{(2)}_{j_k+m_k,j_k+m_k+1} \times \Delta d^{*}_{j_k+m_k,j_k+m_k+1} \right) = 0 \end{aligned} \tag{A.6}$$

At this point, $W(\phi) \geq 0$. In addition, $W(t)$ is continuous for $t \in [0, \phi] \subset (0, +\infty)$, so that at least one real root $\xi \in (0, \phi]$ that satisfies $W(\xi) = 0$. Thus, this corollary is proven.

References

[1] Hannes Hartenstein and Kenneth P Laberteaux. A tutorial survey on vehicular ad hoc networks. *Communications Magazine, IEEE*, 46(6):164–171, 2008.

[2] Ekram Hossain, Garland Chow, Victor Leung, Robert D McLeod, Jelena Mišić, Vincent WS Wong, and Oliver Yang. Vehicular telematics over heterogeneous wireless networks: A survey. *Computer Communications*, 33(7):775–793, 2010.

[3] Greg Marsden, Mike McDonald, and Mark Brackstone. Towards an understanding of adaptive cruise control. *Transportation Research Part C: Emerging Technologies*, 9(1):33–51, 2001.

[4] Ardalan Vahidi and Azim Eskandarian. Research advances in intelligent collision avoidance and adaptive cruise control. *Intelligent Transportation Systems, IEEE Transactions on*, 4(3):143–153, 2003.

[5] Rajesh Rajamani. Adaptive cruise control. In *Vehicle Dynamics and Control*, pages 141–170. Springer, 2012.

[6] James A Misener and Steven E Shladover. Path investigations in vehicle-roadside cooperation and safety: A foundation for safety and vehicle-infrastructure integration research. In *Intelligent Transportation Systems Conference, IEEE*, pages 9–16. IEEE, Sep 2006.

[7] Petros Ioannou, Yun Wang, and Hwan Chang. *Integrated roadway/adaptive cruise control system: Safety, performance, environmental and near term deployment considerations.* California PATH Program, Institute of Transportation Studies, University of California at Berkeley, 2007.

[8] Todd Spangler and Detroit Free Press. Feds move to require car-to-car safety communication. http://www.usatoday.com/story/money/cars/2014/02/03/nhtsa-vehicle-to-vehicle-communication/5184773/, Feb 2013.

[9] Animesh Chakravarthy, Kyungyeol Song, and Eric Feron. Preventing automotive pileup crashes in mixed-communication environments. *Intelligent Transportation Systems, IEEE Transactions on*, 10(2):211–225, 2009.

[10] Louis A Pipes. An operational analysis of traffic dynamics. *Journal of applied physics*, 24(3):274–281, 1953.

[11] Robert E Chandler, Robert Herman, and Elliott W Montroll. Traffic dynamics: studies in car following. *Operations research*, 6(2):165–184, 1958.

[12] Arnab Bose and Petros Ioannou. Mixed manual/semi-automated traffic: a macroscopic analysis. *Transportation Research Part C: Emerging Technologies*, 11(6):439–462, 2003.

[13] Arnab Bose and Petros A Ioannou. Analysis of traffic flow with mixed manual and semiautomated vehicles. *Intelligent Transportation Systems, IEEE Transactions on*, 4(4):173–188, 2003.

[14] Carolina Garcia-Costa, Esteban Egea-Lopez, Juan Bautista Tomas-Gabarron, Joan Garcia-Haro, and Zygmunt J Haas. A stochastic model for chain collisions of vehicles equipped with vehicular communications. *Intelligent Transportation Systems, IEEE Transactions on*, 13(2):503–518, 2012.

[15] Carolina García-Costa, Esteban Egea-López, and Joan García-Haro. A stochastic model for design and evaluation of chain collision avoidance applications. *Transportation Research Part C: Emerging Technologies*, 30:126–142, 2013.

[16] Datta N Godbole and John Lygeros. Longitudinal control of the lead car of a platoon. *Vehicular Technology, IEEE Transactions on*, 43(4):1125–1135, 1994.

[17] D Swaroop and JK Hedrick. String stability of interconnected systems. *Automatic Control, IEEE Transactions on*, 41(3):349–357, 1996.

[18] DVAHG Swaroop. String stability of interconnected systems: An application to platooning in automated highway systems. 1997.

[19] Jing Zhou and Huei Peng. Range policy of adaptive cruise control vehicles for improved flow stability and string stability. *Intelligent Transportation Systems, IEEE Transactions on*, 6(2):229–237, 2005.

[20] Woosuk Choi and Darbha Swaroop. Assessing the safety benefits due to coordination amongst vehicles during an emergency braking maneuver. In *American Control Conference*, pages 2099–2104. IEEE, Jun 2001.

[21] Woosuk Choi and S Darbha. Assessing the benefits of coordination in automatically controlled vehicles. In *Intelligent Transportation Systems*, pages 70–75. IEEE, Aug 2001.

[22] Antony Tang and Alice Yip. Collision avoidance timing analysis of dsrc-based vehicles. *Accident Analysis & Prevention*, 42(1):182–195, 2010.

[23] Daniel Jiang, Vikas Taliwal, Andreas Meier, Wieland Holfelder, and Ralf Herrtwich. Design of 5.9 ghz dsrc-based vehicular safety communication. *Wireless Communications, IEEE*, 13(5):36–43, 2006.

[24] T. Taleb, A. Benslimane, and K. Ben Letaief. Toward an effective risk-conscious and collaborative vehicular collision avoidance system. *Vehicular Technology, IEEE Transactions on*, 59(3):1474–1486, 2010.

[25] S. Biswas, R. Tatchikou, and F. Dion. Vehicle-to-vehicle wireless communication protocols for enhancing highway traffic safety. *Communications Magazine, IEEE*, 44(1):74–82, 2006.

[26] P. Tientrakool, Ya-Chi Ho, and N.F. Maxemchuk. Highway capacity benefits from using vehicle-to-vehicle communication and sensors for collision avoidance. In *Vehicular Technology Conference (VTC Fall), IEEE*, pages 1–5, Sep 2011.

[27] Han Cai and Do Young Eun. Crossing over the bounded domain: from exponential to power-law inter-meeting time in mobile ad hoc networks. *Networking, IEEE/ACM Transactions on*, 17(5):1578–1591, 2009.

[28] Stratis Ioannidis, Augustin Chaintreau, and Laurent Massoulié. Optimal and scalable distribution of content updates over a mobile social network. In *INFOCOM*, pages 1422–1430. IEEE, Apr 2009.

[29] Hongzi Zhu, Luoyi Fu, Guangtao Xue, Yanmin Zhu, Minglu Li, and Lionel M Ni. Recognizing exponential inter-contact time in vanets. In *INFOCOM*, pages 1–5. IEEE, Mar 2010.

[30] Yong Li, Zhaocheng Wang, Depeng Jin, Li Su, Lieguang Zeng, and Sheng Chen. Optimal beaconing control

for epidemic routing in delay-tolerant networks. *Vehicular Technology, IEEE Transactions on*, 61(1):311–320, 2012.

[31] Harvard University. Erskine Bureau for Street Traffic Research, Harry Reginald De Silva, and Theodore Watson Forbes. *Driver testing results*. 1937.

[32] RD Lister. The reaction time of drivers in moving and stationary vehicles, 1950.

[33] DG Liebermann, G Ben-David, N Schweitzer, Y Apter, and A Parush. A field study on braking responses during driving. i. triggering and modulation. *Ergonomics*, 38(9):1894–1902, 1995.

[34] Lora Warshawsky-Livne and David Shinar. Effects of uncertainty, transmission type, driver age and gender on brake reaction and movement time. *Journal of safety research*, 33(1):117–128, 2002.

[35] Daniel B Fambro, Kay Fitzpatrick, and Rodger J Koppa. New stopping sight distance model for use in highway geometric design. *Transportation Research Record: Journal of the Transportation Research Board*, 1701(1):1–8, 2000.